Available online at www.sciencedirect.com
SCIENCE DIRECT®
International Journal of Mass Spectrometry 235 (2004) 59–81
International Journal of Mass Spectrometry
www.elsevier.com/locate/ijms

Multidynamic isotope ratio analysis using MC–ICP–MS and the causes of secular drift in Hf, Nd and Pb isotope ratios

M.F. Thirlwall [a,*], R. Anczkiewicz [a,b]

[a] *Department of Geology, Royal Holloway University of London, Egham, Surrey TW20 0EX, UK*
[b] *Department of Geological Sciences, University College London, Gowar Street, London WC1E 6BT, UK*

Received 8 December 2003; accepted 1 April 2004

Abstract

The causes of secular drift in multicollector (MC)–ICP–MS normalized isotope ratios were investigated using multidynamic measurements of Nd, Yb, Hf and Pb isotope ratios over 2.5 year on an IsoProbe MC–ICP–MS, and of Nd and Yb by thermal ionisation mass spectrometry (TIMS). We present the first TIMS multidynamic determinations of all nonradiogenic Nd isotope ratios, which differ significantly from previously assumed reference values. Multidynamic isotope ratios measured on the IsoProbe show much less secular drift than static ratios calculated from the same mass spectrometer runs, and for example improve Hf external precision to ~60 to 75 ppm 2S.D. for all ratios. The poor performance of static measurements cannot easily be attributed to Faraday cup deterioration because static data show cyclic and sometimes rapid secular drift. Multidynamic Nd and Yb ratios, normalized using exponential law, show systematically greater deviation from TIMS ratios the greater the difference in average mass between normalized and normalising ratios. Nearly accurate isotope ratios for Yb and for two of three sets of Nd data can be calculated using a general power law (GPL) with exponent of −0.63. This implies that our multidynamic $^{176}Hf/^{177}Hf$ and $^{180}Hf/^{177}Hf$ ratios, and those reported by most other laboratories also using normalisation by exponential law to $^{179}Hf/^{177}Hf = 0.7325$, are lower than the true isotope ratios. General power law normalisation does not reduce secular variation in multidynamic ratios. Correlations between ratios normalized by exponential or general power law can only partly be explained by variation in the general power law exponent from day to day. Exponential-law normalized $^{143}Nd/^{144}Nd$, $^{142}Nd/^{144}Nd$ and $^{145}Nd/^{144}Nd$ lie within error of a plane in three dimensions: empirical correction of $^{143}Nd/^{144}Nd$ using this plane yields 25 ppm external precision (2S.D.) for all multidynamic $^{143}Nd/^{144}Nd$ over 2.5 years and results in a corrected ratio identical to TIMS. Linear regressions for Hf isotope ratios yield 50 ppm 2S.D. on $^{176}Hf/^{177}Hf$ over the same period. Algorithms are presented for static and multidynamic analysis of spiked Nd and Hf samples and we show that these yield the same nonradiogenic ratios as standard samples despite a wide range of matrix types.

Keywords: MC–ICP–MS; TIMS; Mass bias; Multidynamic; Hf; Nd; Yb

1. Introduction

Multicollector inductively-coupled plasma mass spectrometry (MC–ICP–MS) is now commonly used for routine isotope ratio measurement of elements that show natural isotopic variability as a result of radioactive decay or of natural mass fractionation processes. For the former, mass bias correction is commonly carried out by normalisation to an accepted value for a non-radiogenic ratio of the element itself (e.g. Hf, Nd, Sr) or of a dopant element of similar mass (e.g. Pb using Tl). However, several laboratories have reported that such normalized ratios for standards show secular drift in value (e.g. Nd [1]; Hf [2]; Pb [3]) such that it is common to correct sample data to the mean value of standards run on a given day, or to adjust apparent cup efficiencies on a daily basis until accurate isotope ratios are obtained for standards. Indeed, Albarède [4] has advised using MC–ICP–MS like stable isotope mass spectrometers, with correction to bracketing standards even for elements like Hf and Nd.

While such corrections can undoubtedly yield high quality data, there are several drawbacks. They require measurement of several standard samples over the course of an analytical session in order to characterise the day's standard mean, and more to characterise any drift that may exist during the course of the analytical session. The standard is then of little

* Corresponding author. Tel.: +44-178-444-3609; fax: +44-178-447-1780.
E-mail address: m.thirlwall@gl.rhul.ac.uk (M.F. Thirlwall).

1387-3806/$ – see front matter © 2004 Elsevier B.V. All rights reserved.
doi:10.1016/j.ijms.2004.04.002

use for determining long-term reproducibility, and analyses of a secondary standard may also be required to assess this. The uncertainty on the standard analyses and on any drift in a given day should be compounded with sample errors, and there is no indication in the literature that this has been done. Secular drift occurs not just in the radiogenic ratios but also in nonradiogenic ratios such as $^{180}Hf/^{177}Hf$ and $^{150}Nd/^{144}Nd$, whose accuracy in samples spiked for isotope dilution analysis may control the accuracy of the element concentration. Finally, there is no absolute guarantee that the process causing drift in standard isotope ratios will cause the same drift in sample ratios: for example, apparent drift could be caused by contamination of a standard solution.

In view of these issues, it is obviously important to try to understand the causes of secular variation and thereby attempt to minimise it. Two main causes have been proposed: that fluctuations in the plasma cause variation in relative ion transmission to the collectors that can be accounted for by changing cup efficiencies [1] and/or that mass bias is not adequately described by simple mass bias laws, and that the exact form of the mass bias law can change on a daily basis (e.g. [5,6]). The existence of secular variation also raises the question of whether accurate isotopic ratios can be determined by MC–ICP–MS. This is usually judged through comparison with thermal ionisation mass spectrometry (TIMS), but the TIMS data for Hf is very imprecise compared with MC–ICP–MS Hf data, while the commonly-used comparative TIMS Nd data is single collector NdO^+ data possibly with substantial uncertainty resulting from the oxygen corrections [7].

In this paper we investigate the causes of drift in MC–ICP–MS isotope ratios using multidynamic isotope analysis of Hf, Yb, Nd and Pb on a Micromass (now GV Instruments) IsoProbe MC–ICP–MS and for the latter three elements using a VG354 TIMS. We also report methodology for Hf and Nd ratio recovery from spiked samples, including multidynamic spiked analyses. We observe substantial drift with time in static Hf, Nd and Pb isotope ratios that is much reduced using multidynamic data. Multidynamic Hf ratios show correlations similar to but less extensive than those shown by Nd ([5], this paper) suggesting that secular multidynamic drift is largely caused by variations in the extent of non-exponential mass bias. A comparison of TIMS and IsoProbe Yb isotope ratios shows that the magnitude of non-exponential mass bias on our IsoProbe is similar for Yb and Nd, and is therefore likely to be the same for Hf. This requires that the true $^{176}Hf/^{177}Hf$ of JMC475 standard (assuming $^{179}Hf/^{177}Hf = 0.7325$) is significantly higher than that reported by most laboratories.

2. Analytical details

2.1. Materials

All reagents used were sub-boil distilled in Teflon, with water being >18 MΩH_2O from a Millipore Element plant. JMC475 Hf isotope standard solution was kindly provided by Prof. J. Patchett, and was diluted with 2% HNO_3:0.1% HF to ∼100 ppb for analysis. The 1000 ppm atomic absorption standard solutions from Aldrich Chemicals were diluted with 2% HNO_3 to ∼100 ppb for Nd and Yb IsoProbe analysis (batches 00307TK and 05021CM, respectively). Rock and mineral samples for IsoProbe Hf–Nd analysis were prepared using the chemical separation methods of [36]. For TIMS analysis 5–10 μL of each Aldrich solution were loaded onto the Ta side filaments of a Ta side Re centre triple filament assembly, previously degassed at 5.2 A on all filaments for 5 min. Standard reference materials SRM981 and SRM982 (US National Institute of Science and Technology) and ^{207}Pb–^{204}Pb double spike solutions were prepared for multidynamic IsoProbe Pb analysis as described in [8].

2.2. Instruments

MC–ICP–MS analyses used a Micromass (now GV Instruments) IsoProbe, with similar instrument settings to [8], and all sample solutions were introduced using a Cetac Aridus fitted with CPI PFA nebulizers with sample uptake of either ∼60 or ∼120 μL min^{-1}, giving sensitivity around $1.5–3 \times 10^{-9}$ A/ppm Hf, Nd or Yb. Sample consumption was 10–80 ng for a static multicollector analysis and 40–200 ng for a multidynamic analysis. Between samples the inlet system was cleaned with 5% HNO_3 followed by 5% HNO_3–5% HF after a Hf analysis, which always extracted much more Hf from the inlet system. Subsequently, 2% HNO_3 was aspirated and used to measure on-peak zeroes (OPZ) for Nd or Yb, while 2% HNO_3–0.1% HF was used for Hf. Following an interface upgrade in March 2002, the option of operating in hard or soft extraction mode was introduced. In the latter ions are transmitted into the mass spectrometer with a slight positive potential between extraction and skimmer cones, which leads to very low memory signals but about 60% less sensitivity.

TIMS analyses used the VG354 5-collector mass spectrometer used by Thirlwall [9] for Sr–Nd isotope analyses. This paper described deterioration of the Faraday cups over ∼6-month periods resulting in drift in multidynamic Sr–Nd data, but this has been overcome by changes to Faraday cup design [10] and our multidynamic $^{87}Sr/^{86}Sr$ and $^{143}Nd/^{144}Nd$ data have been reproducible to ±0.000014 and ±0.000007, respectively (2S.D., $N > 200$ for Sr, $N > 100$ for Nd, only 1.4× typical internal precision) for the last 4 years, which includes the period of this study. Both Yb and Nd were run as metal ion species.

2.3. Collectors

Collector set ups were identical for both multidynamic and static runs, and are listed in Table 1. All Faradays used 10^{11} Ω resistors. All multidynamic runs involved three

Table 1
Collector set up for static and multidynamic Hf, Nd and Yb isotope analysis

Hf	L3	L2	Ax	H1	H2	H3	H4	H5	H6
Jump 1	171	173	174	175	*176*	177	178	179	181
Jump 2[a]	172	174	175	176	*177*	178	179	180	182
Jump 3	173	175	176	177	*178*	179	180	181	183
Nd	L3	L2	Ax	H1	H2	H3	H4	H5	H6
Jump 1		141	142	*143*	144	145	146	148	149
Jump 2[a]	140	142	143	*144*	145	146	147	149	150
Jump 3		143	144	*145*	146	147	148	150	
Nd TIMS1		L2	L1	Ax	H1	H2			
Jump 1		140	142	*143*	144	146			
Jump 2		141	143	*144*	145	147			
Jump 3		142	144	*145*	146	148			
Nd TIMS2		L2	L1	Ax	H1	H2			
Jump 1		142	*143*	144	*146*	148			
Jump 2		143	*144*	145	*147*	149			
Jump 3		144	*145*	146	*148*	150			
Yb	L3	L2	Ax	H1	H2	H3	H4	H5	H6
Static REE	155[b]	159[b]	164[b]	171	172	174	175	176	177
Static Yb-Hf		170	171	172	173	177	178	179	180
Multidynamic									
Jump 1	167	169	170	171	*172*	173	174	175	
Jump 2	168	170	171	172	*173*	174	175	176	
Jump 3	169	171	172	173	*174*	175	176	177	
TIMS cups			L2	L1	Ax	H1	H2		

Italics signifies the masses that were centered for each jump. Two sets of data were collected on NdTIMS2, centered in L1 and H1.

[a] Jump 2 is the collector configuration also used for static analysis.

[b] Used to make interference corrections for Gd, Tb and Dy oxides and hydroxides on Yb and Lu masses during rare earth element (REE) analysis.

magnetic field jumps, with the collectors aligned to the masses shown in jump 2. Solutions (IsoProbe) or beads (TIMS) containing the interfering elements were used to ensure perfect alignment. A fourth jump was used in TIMS runs to permit measurement of a half-mass baseline. The jump 2 alignment was also used to calculate ratios on static runs, and to calculate pseudo-static ratios in multidynamic runs for direct comparison to the multidynamic ratios. The Hf set up permits static measurement of all Hf isotope ratios, while the Nd IsoProbe set up is the same as used by [5]. The first Nd TIMS setting is the same as used by [9], apart from collector H2 being used for ^{148}Nd measurement, while the second TIMS set up allows multidynamic measurement of ^{150}Nd. Yb was analysed using several static collector configurations on the IsoProbe, either as part of a rare earth element (REE) isotope dilution procedure, or in various mixtures with Lu and Hf. The multidynamic Yb set up was the same on the IsoProbe as on TIMS, although the fewer collectors available on our TIMS machine mean that no in-run monitoring of potential Er and Hf interferences took place.

3. Data processing

For TIMS runs, ratios were calculated on-line using modifications of the original instrument software. Baselines were measured in a fourth multidynamic jump at a single half-mass position and subtracted from all peak intensities. For the IsoProbe, amplifier voltages, corrected only for electronic gain, were transferred to Microsoft excel and processed off-line using similar principles to the Pb study of [8].

3.1. On-peak zeroes (IsoProbe only)

On-peak zeroes were determined on the 2% HNO_3 (Nd, Yb, Pb) or 2% HNO_3–0.1% HF (Hf) used to dissolve the samples, using about 0.7*N* static integrations or 0.7*N* multidynamic cycles where *N* integrations or cycles were used for the sample measurements. Fewer OPZ than this unacceptably worsens precision on the low-intensity isotopes. As described by [8], OPZ correct for amplifier baseline, blank Hf, Yb, Nd, Sm, etc. in the dilute acid solution used, and memory of these and other components in the inlet system and mass spectrometer. Raw OPZ data are inspected for drift and pulses from previous samples prior to placing the Aridus uptake capillary into the sample solution. For Hf, the latter mostly appear to result from microparticulate fluorides in the spray chamber as rinsing this out removes the effect. If substantial pulsing is observed, the OPZ measurement is re-run. Means and 2S.E. values of OPZ intensities are pasted into the sample data file and subtracted from individual sample peak integrations, and OPZ 2S.E. values are used in propagating uncertainties on the ratios. Each day, amplifier offsets are measured with no ion beam in the analyser (mass spectrometer zeroes or MSZ) and their means and 2S.E. values are also pasted into the sample data file. They are only used to determine mean peak intensities for the blank solution by subtraction from mean OPZ intensities for each mass.

These memory signal intensities vary from <0.05fA to a maximum of 7fA ^{180}Hf, 12fA ^{172}Yb and 20fA ^{142}Nd (e.g. Fig. 1). Memory for Pb was as described by [8]. Very low memory signal intensities are observed in soft extraction mode (<0.6fA ^{180}Hf and ^{142}Nd and <0.15fA ^{172}Yb). Hf and Nd relative abundances in the memory signal are broadly similar to natural, and have little impact on measured isotope ratios even at the maximum memory of 20fA ^{142}Nd in hard extraction. However, memory intensities in hard extraction at masses 172–176 are not consistent with Yb–Lu–Hf mixtures, with 173 and 172 intensities being subequal, inconsistent with $^{173}Yb/^{172}Yb = 0.7362$.

In principle unidentified molecular ions in the memory should not cause a problem in Hf isotopic analysis, provided that their intensities remain constant and that the sample solution does not extract any more (or less) of these moleculars than the blank solution used for OPZ measurement. These assumptions are tested by whether the OPZ signal remains constant between samples and by whether

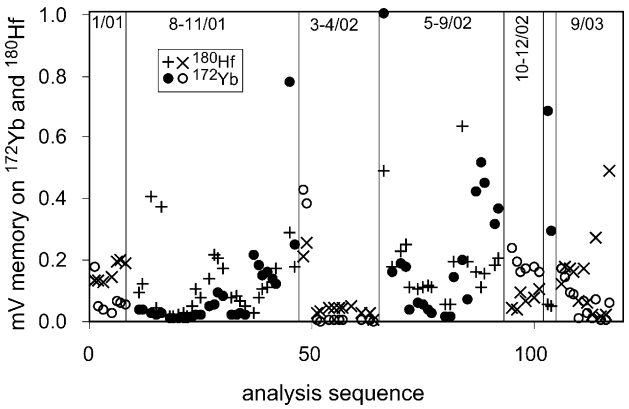

Fig. 1. Memory intensities (1 mV = 10 fA) of ^{172}Yb and ^{180}Hf from multidynamic runs of JMC475 standard between January 2001 and September 2003. Note contrast between hard (first two analyses) and soft extraction (the remainder) in period 3–4/02.

^{173}Yb/^{172}Yb ratios are consistent with natural Yb during sample runs. For a few Hf runs the mass 172 OPZ was observed to change by up to 50% between runs, and after OPZ correction the 173 intensity in multidynamic runs was frequently observed to be 0.08–0.15fA compared with ±0.05fA at mass 172. This would however only lead to an inaccuracy of ∼0.000008 in ^{174}Hf/^{177}Hf. During one analytical session, we observed variable negative signals at mass 172 and 173 after OPZ subtraction, suggesting that under some circumstances both Hf samples and standards can extract less of these moleculars from the instrument than the blank solution.

To counter this problem we have used three strategies:

- The option is available to use the time interpolated mean of OPZ measurements made before and after the sample analysis. This counters drift in OPZ signal intensities.
- We determine ^{174}Hf/^{177}Hf for each sample run. Since ^{174}Hf is a minor isotope of Hf but a major isotope of Yb, this is highly sensitive to any problem with the Yb interference correction. For the few runs in which mass 172 OPZ changes significantly between runs, the ^{174}Hf/^{177}Hf ratios are much closer to normal if a time-interpolated OPZ is used rather than just the pre-analysis OPZ.
- Data from hard extraction runs can be compared with those run with soft extraction, where there is almost no detectable memory at REE masses. There is no difference in ^{174}Hf/^{177}Hf. Unfortunately, with our current interface configuration there is a 3× sensitivity penalty in soft extraction which precludes its routine use for other than large samples. A new interface pumping design that yields high sensitivity in soft extraction is currently under test at GV Instruments Ltd.

3.2. Tail corrections

No tail correction was necessary for TIMS analyses where <1 ppm of the ^{142}Nd peak was observed at −1 amu. Thirlwall [8,11] showed that correction for overlap of adjacent peaks up to 3 amu away is essential for accurate isotope ratio analysis of heavy elements on the Royal Holloway IsoProbe, and described the use of Bi to determine the tail profile for Pb. For Hf and Yb, tails are measured each analytical session using a 90 pA signal of ^{181}Ta, for which the very small ^{180}Ta signal is too small to have significant effect on the measured tail profile. The profile is most conveniently measured by a slow scan from mass 176.5–185.5, with tails at ±1, ±2 and ±3 amu interpolated from the scan and averaged across the collector array. Typical tail values for Hf are listed in Table 2, and are subtracted from peak intensities is the way described in [11].

3.3. Crosstalk

Correction for "crosstalk" was described by [12], but it was first discovered during Hf analysis, and the correction has been retrospectively applied to all other analyses. Prior to making the crosstalk correction, it was discovered that mean intensities at masses 172, 173 and 175 on Hf runs were significantly greater than zero after correcting for OPZ and tail. This was true even on pure solutions of JMC475 Hf standard which should contain no Yb or Lu. The absence of Yb and Lu from the JMC475 Hf solution was confirmed by comparing a scan over these peaks on the Daly electron multiplier on the blank solution used for OPZ measurement with a similar scan across JMC475 solution.

With ∼70 pA ^{180}Hf, mean OPZ and tail corrected intensities observed at masses 172 and 175 were around 0.3–0.5 fA, equivalent to ^{172}Yb/^{177}Hf ratios of ∼0.000011. Clearly these signals cannot be real HREE ion signals, both because of their absence from Daly scans and because they suggest ^{173}Yb/^{172}Yb ∼ 1 when the natural ratio is 0.736. Extensive experiments with monoisotopic ^{232}Th solutions at ∼90 pA ^{232}Th showed that after correction for OPZ and tail there was a constant signal observed on all the other Faraday amplifiers of ∼0.22 fA. This was observed whatever collector was used to integrate ^{232}Th and wherever the other Faraday buckets were physically located relative to the ^{232}Th beam e.g. set to unit or part-mass spacings. The signal was not observed on the Daly multiplier. We interpret it as resulting from electronic crosstalk between Faraday amplifiers; however, we have replaced the amplifier boards and observed no difference. Whatever its cause, a subtraction

Table 2
Typical tail values for Hf at ±1 to 3 amu from ^{181}Ta, measured as ppm of ^{181}Ta

amu	ppm
−3	2
−2	5
−1	15
+1	10
+2	3
+3	0

These values correspond to an abundance sensitivity of ∼22 ppm at ^{238}U.

from each Faraday intensity of 2.5 ± 0.2 ppm of the sum of all measured Faraday intensities produces 172, 173 and 175 signals within error of zero except where Yb and Lu are present on Daly scans. Crosstalk is <1 ppm on our TIMS.

3.4. Faraday dynamic memory

In multidynamic routines, care must be taken to correct adequately for the finite time taken for ion signals to decay on the Faraday amplifiers. To compensate, there is usually a time delay between setting the magnet and commencing ion integration, and the subsequent ion signal is corrected for any remaining decay of the previous signal through hardware "tau" corrections. For the TIMS analyses reported here, integration times of 5 s and delay times of 3.5 s were used, and the hardware tau settings were checked by running a Nd sample with a 6.5 s delay time, which showed no significant difference in ratios to that with a 3.5 s delay. IsoProbe multidynamic runs used 10 s integration times and 3 s delay times. IsoProbe hardware tau settings were checked using Gd, with which it is possible to measure Faraday time constants in five Faraday detectors simultaneously, using >50 pA ion beams of masses 155, 156, 157, 158 and 160. To mimic the IsoProbe multidynamic runs, the Gd ion beams were integrated for 10 s, then a jump was made to a half-mass position, and during a 3 s delay at this field, the analyser isolation valve was closed manually. The field jump alone would have been inadequate to measure dynamic memories, as the ion signal at half-mass positions is dominated by peak tails [11]. Three successive 10 s integrations separated by 3 s delays were then made at this field, and during the final delay period the isolation valve was opened in time for a return to the Gd peaks. The residual dynamic memory after the hardware correction was found to be 1.5–6 ppm for the first 10s integration, dropping to <2 ppm on the second.

3.5. Interferences and their correction

Following the corrections listed above, raw static ratios are calculated with ^{172}Yb, ^{144}Nd($\pm^{144}$Sm) or ^{177}Hf as the denominator isotope. These ratios may be affected by interference from molecular ions or simple elemental isobars. It is very difficult to predict all possible molecular interferences: our strategy is to use OPZ measurements to correct for any moleculars generated in the instrument in the absence of sample, and to use the similarity between non-radiogenic ratios of standards and real samples as evidence that any moleculars generated by the sample are insignificant. Potential moleculars include oxides, hydrides, hydroxides, nitrides and argides. Oxides, hydrides and hydroxides are reduced by using the Aridus desolvating nebulizer, and Gd, Tb and Dy oxides and hydroxides, which could potentially interfere with Hf and Yb analyses, are routinely measured during Yb and Lu analysis by isotope dilution (Table 1, REE settings). Hydride production is effectively removed by the tail correction, and must be <∼1 ppm. Oxide production rates for Gd, Tb and Dy are typically 0.5, 0.3 and 0.04%, respectively; hydroxide production rates are typically 0.1% for Gd and <0.01% for Tb and Dy. For all sample Hf runs reported here, Yb^+ ion beams are so low that these oxide and hydroxide interferences are insignificant. During Nd analysis, Ba is the only sample impurity likely to generate significant interfering oxide or hydroxide moleculars. Experiments with Ba solutions suggest that their production rates are very low (0.014% BaO^+ and 0.033% $BaOH^+$), and only produce problems with unradiogenic ratios for >100 pA ^{138}Ba ion beams. Nitride moleculars have not been clearly observed, and argide moleculars are suppressed by the IsoProbe hexapole. In principle Ba might generate argides that would interfere with Hf analyses, but we have observed nothing detectable on a Faraday detector ($BaAr^+$/Ba < 0.003%).

Very small corrections were necessary for isobaric interferences from Er and Hf for the Yb standard analyses on the IsoProbe. Er interference on mass ^{170}Yb was not monitored during TIMS Yb analysis, but a scan at the end of one analysis revealed no significant ^{166}Er peak on a Daly electron multiplier. ^{176}Hf was assumed to be absent at the relatively low filament temperatures used for Yb analysis. For Nd, ^{147}Sm was used to correct Sm interferences assuming the Sm isotope ratios of [7] for natural samples, and using iteratively calculated ratios based on ^{147}Sm/^{149}Sm for spiked samples (Section 3.7). Ce corrections used ^{142}Ce/^{140}Ce = 0.125 on the TIMS, and between 0.12584 and 0.12598 on the IsoProbe, which were determined as the ratios needed to yield the same ^{142}Nd/^{144}Nd on Ce-spiked as Ce-free Nd standard solutions on the same day as the sample analyses. On the IsoProbe, both Sm and Ce natural ratios were adjusted to the mass bias of Nd observed in each integration, using an iterative solution to ^{146}Nd/^{144}Nd. Aldrich Nd solutions spiked to Sm/Nd = 0.2 yielded the same Nd ratios as Sm-free Nd within our normal standard precision. Hg corrections on ^{204}Pb were carried out using both ^{201}Hg and ^{202}Hg [8]; multidynamic runs allow the measurement of several natural Hg isotope ratios.

For Hf, isobaric interference corrections are made on masses 174, 176 and 180 using ^{172}Yb, ^{175}Lu and ^{182}W, which are measured simultaneously in static runs and in jump 2 of multidynamic runs. ^{181}Ta, to correct mass 180, is measured in jump 3 of multidynamic runs or using a single integration outside the run for static analyses. For most of the multidynamic data presented here ^{176}Hf and ^{174}Hf in jumps 1 and 3 of multidynamic runs were corrected for Yb and Lu based on the observed ^{172}Yb/^{177}Hf and ^{175}Lu/^{177}Hf from jump 2. We have observed occasional transient pulses of Yb and Lu during sample runs suggesting that the correction should instead be based on simultaneous measurements of Yb and ^{175}Lu, and this method was used for data collected after Jan. 2003. ^{180}Hf is not analysed simultaneously with ^{181}Ta or ^{182}W in jumps 2 and 3, respectively of multidynamic runs. Here, the corrections are based on ^{181}Ta/^{177}Hf and ^{182}W/^{177}Hf measured in other jumps.

For all corrections to Hf the natural abundance ratios of Yb, Lu, W and Ta were adjusted to the observed Hf mass bias, calculated from the $^{179}Hf/^{177}Hf$ of each integration, iteratively for spiked samples. Natural $^{180}W/^{182}W$ was determined as that natural ratio that yielded identical multidynamic $^{180}Hf/^{177}Hf$ on W-spiked JMC475 solution to that of bracketing W-free solution. This value was 0.004450, similar to the 0.00449 reported by Harper et al. [13]. $^{180}Ta/^{181}Ta$ is taken to be 0.000115 [14]: this is so low that uncertainty in the ratio has insignificant effect on ^{180}Hf.

Yb isotope ratios determined on TIMS [15] were adopted by Blichert-Toft et al. to [16] make interference corrections on Hf, but have since been questioned by [17,18]. Chu et al. [17] assumed that the initial mass bias shown by Yb standards during TIMS analysis was similar to that shown by Nd and Ce standards loaded onto filaments in the same way, and suggested that natural Yb was 0.4% amu^{-1} more enriched in heavy isotopes than [15]. Apparently different Yb ratios were reported by [18], in which MC–ICP–MS was used to determine a 'true' value for $^{171}Yb/^{172}Yb$ by normalising independently to $^{179}Hf/^{177}Hf = 0.7325$ and to an absolute TIMS determination of $^{166}Er/^{167}Er$ made by gravimetric methods [19]. Their 'true' $^{171}Yb/^{172}Yb$ was subsequently used to normalise other Yb ratios. Neither [17] nor [18] quoted errors on their final Yb ratios that incorporated the uncertainties in the normalising ratios. For the Chu et al. [17] method, this would appear to be about 0.1% amu^{-1} based on the range of $^{146}Nd/^{144}Nd$ in their TIMS work. The uncertainty on the $^{166}Er/^{167}Er$ normalising ratio used by [18] can be estimated as ±0.04% 2 S.D. amu^{-1} using the data of [19]. These propagate to about ±0.05 to ±0.1% uncertainties on $^{171}Yb/^{172}Yb$ and imply that the two sets of Yb ratios of [17,18] are probably within error. Using a similar approach to [17], our TIMS analyses suggest that the true value of $^{174}Yb/^{172}Yb$ is in the range 1.459 to 1.462, substantially higher than the 1.451979 proposed by [15]. We have also analysed mixed Yb–Hf solutions on the IsoProbe which suggest $^{174}Yb/^{172}Yb = 1.4618$ through normalisation to $^{179}Hf/^{177}Hf = 0.7325$ (Table 3). The difference in natural $^{176}Yb/^{172}Yb$ and $^{174}Yb/^{172}Yb$ between [15,17] would have no significant effect on $^{176}Hf/^{177}Hf$ for $^{172}Yb/^{177}Hf < 0.0005$, but would cause detectable differences in $^{174}Hf/^{177}Hf$ for $^{172}Yb/^{177}Hf > 0.0002$. $^{172}Yb/^{177}Hf$ was <0.00005 for the vast majority of standards and samples discussed here. Five multidynamic JMC475 were run with $^{172}Yb/^{177}Hf =\sim 0.0011$ due to a Yb-contaminated centrifuge tube: these yielded $^{174}Hf/^{177}Hf \sim 0.000012$ higher than in Yb free runs using corrections to the Yb ratios of [15], but identical values using the Yb ratios of [17].

3.6. Ratio calculations: unspiked samples

Final static isotope ratios are calculated in the conventional way using exponential-law normalisation to $^{179}Hf/^{177}Hf = 0.7325$, $^{174}Yb/^{172}Yb = 1.4519785$, $^{146}Nd/^{144}Nd = 0.7219$ and $^{208}Pb/^{206}Pb = 2.1677$ and 1.00016 for SRM981 and 982, respectively. The fact that the true $^{174}Yb/^{172}Yb$ is almost certainly higher is irrelevant for the remainder of this work. The static ratios incorporate correction for amplifier gains, measured using a constant current source overnight, but no correction for differential ion transmission to the collectors (i.e. cup efficiencies were always set to 1). No statistical outlier rejection package was used.

We use the same type of multidynamic algorithms as used for TIMS Sr and Nd analysis by [9], which cancel out cup efficiencies and temporal ion beam fluctuations. The equations do assume that mass bias is stable between the magnet jumps, and we have seen evidence that this is not always the case. Instability in mass bias on the IsoProbe can occur at <10 s frequency, as observed for example by measured $^{179}Hf/^{177}Hf$ ratios that do not vary systematically during the run, but show much worse internal precision than calculated from ion beam size, and correlate strongly with other Hf ratios. This appears to be caused by instability at the nebulizer, perhaps a partial blockage, and results in multidynamic ratios that are less precise than equivalent static ratios.

The basic equations in these algorithms are power law equations using nominal masses, but since mass bias in MC-ICP-MS is thought to follow broadly the exponential law, the power law results must be converted to exponential-law normalisation. For example, we carry out the exponential conversion for Hf using:

$$\left(\frac{^{z}Hf}{^{177}Hf}\right)_{N,\,multi,\,ex} = \left(\frac{^{z}Hf}{^{177}Hf}\right)_{N,\,multi,\,pl} \times \left(\frac{0.7325}{(^{179}Hf/^{177}Hf_{stat})}\right)^{a} \quad (1)$$

where subscripts ex and pl signify exponential and power law, respectively, N signifies normalized, stat signifies the static ratio uncorrected for mass bias, z refers to mass 176, 178 or 180, and

$$a = \frac{\ln(M_z/M_{177})}{\ln(M_{179}/M_{177})} - \frac{(z-177)}{(179-177)} \quad (2)$$

where M_z is the true atomic mass of isotope z. Eq. (1) can also be used to convert to general power law (GPL) normalisation [20], with q as the exponent, by changing Eq. (2) to

$$a = \frac{M_z^q - M_{177}^q}{M_{179}^q - M_{177}^q} - \frac{z-177}{179-177} \quad (3)$$

These conversions assume that any inaccuracy in the static $^{179}Hf/^{177}Hf$ has little impact on the correction: this may be tested by letting $^{179}Hf/^{177}Hf$ have an error equivalent to the total spread in static normalized ratios. For example, a 500 ppm error in the static ratio would propagate to a maximum 6 ppm error in the exponential-law corrected ratios, which is in all cases insignificant. An alternative formulation for exponential-law multidynamic ratios of Nd and Hf was suggested by [1,16], which does not require use of a

Table 3
Results of Yb–Lu isotope analyses of various mixed pure element standards

	$^{168}Yb/^{172}Yb$	$^{170}Yb/^{172}Yb$	$^{171}Yb/^{172}Yb$	$^{173}Yb/^{172}Yb$	$^{174}Yb/^{172}Yb$	$^{176}Yb/^{172}Yb$	$^{176}Lu/^{175}Lu$	N
Mass bias correction to $^{174}Yb/^{172}Yb = 1.4519785$ [15]								
Royal Holloway								
TIMS multidynamic Yb	–	0.139903 ± 07	0.655345 ± 15	0.736251 ± 22	*1.4519785*	0.579397 ± 19	–	7
IsoProbe multidynamic Yb	–	0.139869 ± 10	0.655287 ± 22	0.736264 ± 06	*1.4519785*	0.579327 ± 11	–	6
Mean 2S.E. (multi IsoProbe)	0.000003 static	0.000006	0.000012	0.000008		0.000016		6
Static on multidynamic run	0.005880 ± 03	0.139887 ± 05	0.655280 ± 17	0.736230 ± 09	*1.4519785*	0.579361 ± 16	–	6
Static on mixed HREE$		–	0.655304 ± 48	–	*1.4519785*	0.57929 ± 12	0.02645 ± 7	50–61
Static, Yb–Hf mixtures	–	0.139912 ± 10*	*0.655345*	0.736234 ± 87	–	–	–	9
Comparisons (all static)								
TIMS [17]	0.005882 ± 14	0.13993 ± 3	0.65535 ± 12	0.73634 ± 13		0.57930 ± 16	0.02644^{+}	2–6
IsoProbe [17]	0.005868 ± 41	0.13984 ± 3	0.65529 ± 03	0.73627 ± 04		0.57926 ± 33	–	19
Nu Plasma [18]	0.005883 ± 12	0.13989 ± 3	0.65530 ± 04	0.73621 ± 05		0.57933 ± 04	–	6
Alternative mass bias corrections								
RH IsoProbe static Yb–Hf	–	0.13894 ± 7*	0.65306 ± 16	0.73878 ± 19	(1.46182)	–	–	9
IsoProbe [17]	0.005773 ± 41	0.13871 ± 3	0.65265 ± 03	0.73924 ± 04	1.46370±19	0.58860 ± 33	0.02655^{+}	19
Nu Plasma [18]	0.005813 ± 13	0.13906 ± 3	*0.653367*	0.73838 ± 06	1.46051±19	0.58612 ± 15	–	6

All uncertainties 2S.D.; uncertainty on $^{176}Lu/^{175}Lu$ is large because it incorporates uncertainty from the ^{176}Yb interference correction in solutions with Lu/Yb = 0.2. *N*, no. of analyses in mean; *, no correction made for small ^{170}Er contribution in the Yb and Lu standard solutions. Italicised ratios are assumed normalisation ratios, all normalisation by exponential-law. IsoProbe multidynamic and Yb–Hf mixture data were acquired on a single day; $, static REE collector alignment (Table 1). Samples include pure Yb and Yb–Lu, Yb–Dy and Yb–Lu–Dy–Er mixtures. Constant $^{176}Lu/^{175}Lu = 0.02645$ was used to calculate $^{176}Yb/^{171}Yb$, but day means of $^{176}Yb/^{171}Yb$ were used to calculate $^{176}Lu/^{175}Lu$. Analyses carried out over 1.5 year period; Alternative mass bias corrections: Royal Holloway Yb–Hf mixtures were normalized to $^{179}Hf/^{177}Hf = 0.7325$. Original normalisation of [17] was to $^{173}Yb/^{171}Yb = 1.132685$; errors quoted above were estimated quadratically; +, preferred TIMS value for $^{176}Lu/^{175}Lu$ of [17].

conversion factor based on a static ratio. Their method involves assuming two reference ratios in order to calculate cup efficiencies and therefore cannot test the accuracy of the assumed second reference ratio.

For normalising ratios ${}^{z+2}E/{}^{z}E$ with a 2 amu difference, as used throughout this study to permit simple comparison between the Hf, Nd and Yb systems, it is only possible to write direct multidynamic algorithms for ratios in the range ${}^{z+4}E/{}^{z}E$ to ${}^{z-2}E/{}^{z}E$. Listed below are examples of such equations for numerator isotopes between $z-2$ and $z+4$.

$$z-2,\ \text{e.g.,}: \left(\frac{{}^{170}\text{Yb}}{{}^{172}\text{Yb}}\right)_{\text{N, multi, pl}} = \frac{170_1 \times 174_3}{172_1 \times 172_3 \times 1.4519785} \tag{4}$$

$$z-1,\ \text{e.g.,}: \left(\frac{{}^{176}\text{Hf}}{{}^{177}\text{Hf}}\right)_{\text{N, multi, pl}} \times = \left(\frac{176_1 \times 176_2 \times 179_3}{177_1 \times 177_2 \times 177_3 \times 0.7325}\right)^{0.5} \tag{5}$$

$$z+1,\ \text{e.g.,}: \left(\frac{{}^{178}\text{Hf}}{{}^{177}\text{Hf}}\right)_{\text{N, multi, pl}} = \left(\frac{178_1 \times 178_2 \times 178_2 \times 178_3 \times 0.7325^2}{177_1 \times 177_2 \times 179_2 \times 179_3}\right)^{0.25} \tag{6}$$

$$z+3,\ \text{e.g.,}: \left(\frac{{}^{180}\text{Hf}}{{}^{177}\text{Hf}}\right)_{\text{N, multi, pl}} = 0.7325 \times \left(\frac{180_2 \times 180_3 \times 177_1 \times 0.7325}{179_1 \times 179_2 \times 179_3}\right)^{0.5} \tag{7}$$

$$z+4,\ \text{e.g.,}: \left(\frac{{}^{176}\text{Yb}}{{}^{172}\text{Yb}}\right)_{\text{N, multi, pl}} = \frac{176_3 \times 172_1 \times 1.4519785^2}{174_1 \times 174_3} \tag{8}$$

where the subscripts refer to the field jumps of Table 1, and the equations yield power-law-normalized ratios which may be converted to exponential law using Eq. (1). Strictly, Eqs. (7) and (8) calculate ${}^{180}\text{Hf}/{}^{179}\text{Hf}$ and ${}^{176}\text{Yb}/{}^{174}\text{Yb}$ respectively, so one might think that Eq. (2) should be reformulated for these different denominator masses. However, it can be shown that the two approaches are algebraically equivalent. Eq. (6) is the geometric mean of two multidynamic measurements: only one of these is possible for ${}^{145}\text{Nd}/{}^{144}\text{Nd}$ on the two TIMS Nd cup configurations (Table 1).

Multidynamic ${}^{150}\text{Nd}/{}^{144}\text{Nd}$ cannot be simply calculated using these equations. We have changed the method of calculation from that used by [5] to

$${}^{150}\text{Nd}/{}^{144}\text{Nd}_{\text{N, multi, ex}} = \left(\frac{150_3 \times 146_1 \times 0.241576^2}{0.7219 \times 148_1 \times 148_3}\right) \times \left(\frac{0.241576}{0.7219 \times {}^{148}\text{Nd}/{}^{146}\text{Nd}_{\text{meas}}}\right)^{F1} \tag{9}$$

where $F1 = \ln(M_{150}/M_{148})/\ln(M_{148}/M_{146}) - 1$.

In this we calculate ${}^{150}\text{Nd}/{}^{148}\text{Nd}$ normalized to ${}^{148}\text{Nd}/{}^{146}\text{Nd} = 0.241576/0.7219$, where 0.241576 is our preferred natural ${}^{148}\text{Nd}/{}^{144}\text{Nd}$ TIMS ratio (Table 4). Most importantly, exactly the same equations are used for TIMS and IsoProbe measurements.

3.7. Ratio calculations: spiked samples

We have performed spiked Nd and Hf isotope ratio analyses in both static and multidynamic mode on the IsoProbe, using mixed ${}^{149}\text{Sm}$–${}^{150}\text{Nd}$, ${}^{176}\text{Lu}$–${}^{180}\text{Hf}$ and ${}^{92}\text{Zr}$–${}^{180}\text{Hf}$ spikes, the latter sometimes in tandem with a mixed rare earth element spike containing ${}^{171}\text{Yb}$ and ${}^{176}\text{Lu}$. These introduce several problems for precise isotope ratio analysis:

(1) ${}^{146}\text{Nd}/{}^{144}\text{Nd}$ and ${}^{179}\text{Hf}/{}^{177}\text{Hf}$ in the spikes is significantly higher than the natural ratios, and since mass bias is likely to be best described by the exponential law, an iterative solution is required for the mass bias corrected ${}^{146}\text{Nd}/{}^{144}\text{Nd}$ and ${}^{150}\text{Nd}/{}^{144}\text{Nd}$ or ${}^{179}\text{Hf}/{}^{177}\text{Hf}$ and ${}^{180}\text{Hf}/{}^{177}\text{Hf}$ of the spike:sample mixtures.
(2) As with other laboratories, we observe secular drift in normalized ratios of unspiked standards. Any drift in the values of ${}^{180}\text{Hf}/{}^{177}\text{Hf}$ or ${}^{150}\text{Nd}/{}^{144}\text{Nd}$ needs accounting for.
(3) Accurate correction of ${}^{180}\text{Hf}$ for W and Ta interference and ${}^{150}\text{Nd}$ and ${}^{144}\text{Nd}$ for Sm interference, before the iterative calculation of mass bias, requires that the natural W, Ta and Sm ratios are corrected to the (unknown) mass bias of the sample run. This obviously becomes less important the lower the interferences are.
(4) When mixed ${}^{176}\text{Lu}$–${}^{180}\text{Hf}$ or ${}^{149}\text{Sm}$–${}^{150}\text{Nd}$ spikes are used, the sample ${}^{176}\text{Lu}/{}^{175}\text{Lu}$ or Sm isotope ratios needed for interference corrections are controlled both by the sample:spike ratio for the interfering element and also by the relative proportion of the element derived from sample + spike to that derived from blank that finally is present in the Hf or Nd run. A similar problem exists with ${}^{176}\text{Yb}/{}^{172}\text{Yb}$ in samples containing mixed REE spikes. The problem is most complex for Nd, where Sm interferes with masses used to iteratively correct for mass bias.

Although there are several possible ways of dealing with these issues, the following method deals simply with the first three for Hf, and for all four for Nd. For static Hf analyses three simultaneous equations can be written, but it is more

Table 4
Results of Nd isotopic analyses

	$^{142}Nd/^{144}Nd$	$^{143}Nd/^{144}Nd$	$^{145}Nd/^{144}Nd$	$^{148}Nd/^{144}Nd$	$^{150}Nd/^{144}Nd$	*N*
Royal Holloway multidynamic TIMS (all Aldrich Nd, except NdTIMS1 which includes one JNdi-1 and two JMC Nd; mean $^{143}Nd/^{144}Nd$ is in all cases from Aldrich Nd)						
1994–1995	1.141879 ± 28	0.511421 ± 06	0.348411 ± 05	–	–	23
NdTIMS1 2003	1.141877 ± 15	0.511413 ± 08	0.348408 ± 05	*0.241587 ± 09*	–	6-9
NdTIMS2 2003	*1.141934 ± 72*	*0.511429 ± 06*	*0.348399 ± 04*	0.241576 ± 06	0.236491 ± 10	10
NdTIMS2 2003	1.141868 ± 29	0.511410 ± 02	0.348407 ± 08	*0.241587 ± 06*	*0.236493 ± 10*	4
Literature TIMS data						
Exponential law [7]	1.141876 ± 53	0.512646 ± 13	0.348415 ± 12	0.241587 ± 14	0.236446 ± 09	?
Power law [7]	1.141827	0.512637	0.348417	0.241577	0.236417	?
Static Triton [22]	1.141791 ± 11	0.511953 ± 02	0.348407 ± 04	0.241575 ± 03	0.236431 ± 07	33
Royal Holloway IsoProbe, Aldrich Nd, multidynamic and static on multidynamic runs						
Pre-upgrade	1.14152 ± 06	0.511354 ± 15	0.348417 ± 10	0.241527 ± 17	0.236371 ± 19	29
Soft extraction	1.14149 ± 10	0.511354 ± 23	0.348425 ± 10	0.241515 ± 36	0.236376 ± 19	12
Hard extraction	1.14124 ± 30	0.511273 ± 99	0.348394 ± 39	0.241514 ± 33	0.236298 ± 83	22
Mean 2S.E., all runs	0.000034	0.000008	0.000004	0.000008	0.000010	
Static pre-upgrade	1.14161 ± 25	0.511346 ± 30	0.348410 ± 21	0.241540 ± 53	0.236299 ± 66	29
Static soft extraction	1.14163 ± 40	0.511314 ± 75	0.348414 ± 36	0.241547 ± 46	0.236266 ± 57	12
Literature MC–ICP–MS data (all a JMC Nd)						
Static P54 [1]	–	0.512227 ± 36	0.348418 ± 11	0.241580 ± 31	0.236427 ± 44	77
Dynamic P54 [1]	–	0.512241 ± 12	–	–	0.236447 ± 13	?
Nu Plasma [6]	1.141778 ± 21	0.512263 ± 09	0.348415 ± 05	0.241559 ± 09	0.236386 ± 11	19

All uncertainties 2S.D., except those listed for [7], which were derived by propagating only their stated uncertainty in oxygen ratios. *N*, no. of analyses in mean. All normalisation to $^{146}Nd/^{144}Nd = 0.7219$ by exponential law, except for [7] 'power law' which were renormalized by Wasserburg et al. [7] from their measured ratios to $^{146}Nd/^{144}Nd = 0.7219$ using power law. For [6] 2S.D. is the mean 2S.D. of three analytical sessions. Each Royal Holloway IsoProbe dataset was collected over a time period between 4 months (pre-upgrade) and 1.5 year. Italics indicate non-optimal peak-centring for the italicised ratios. [7] used chondritic Nd, measured as single collector NdO^+; [22] used Ames Nd.

convenient to add a fourth equation defining a parameter *R*:

$$^{180}Hf/^{177}Hf_T = \Phi \times {}^{180}Hf/^{177}Hf_{WTa} \times R^a \quad (10)$$

$$\left(\frac{^{180}Hf}{^{177}Hf}\right)_{WTa} = \frac{^{180}(Hf + W + Ta)}{^{177}Hf} - \frac{^{181}Ta}{^{177}Hf} \times \frac{^{180}Ta}{^{181}Ta} \times R^b - \frac{^{182}W}{^{177}Hf} \times \frac{^{180}W}{^{182}W} \times R^c \quad (11)$$

$$^{180}Hf/^{177}Hf_T = x \times {}^{179}Hf/^{177}Hf_N + y \quad (12)$$

$$R = \frac{^{179}Hf/^{177}Hf_N}{^{179}Hf/^{177}Hf} \quad (13)$$

where subscript *N* refers to the mass bias normalized ratio and subscript WTa refers to the ratio corrected for W and Ta interference. Subscript T signifies the true sample $^{180}Hf/^{177}Hf$ corrected *both* for mass bias and for drift in the mass bias corrected $^{180}Hf/^{177}Hf$ of unspiked standards. The latter is expressed by Φ, which is equal to $(^{180}Hf/^{177}Hf_{true,\ natural})/(^{180}Hf/^{177}Hf_{observed,\ natural})$. *R* is defined by Eq. (13) and is equivalent to $(M_{179}/M_{177})^{\beta}$, where β is the exponential mass bias coefficient. Exponents *a*, *b*, *c* are mass coefficients defined according to the preferred form of the mass bias law. For the exponential law, $a = \ln(M_{180}/M_{177})/\ln(M_{179}/M_{177})$; $b = -\ln(M_{180}/M_{181})/\ln(M_{179}/M_{177})$ and $c = -\ln(M_{180}/M_{182})/\ln(M_{179}/M_{177})$ where M_z is the atomic mass of *z*. Eq. (12) is the spike-natural mixing equation, and *x* and *y* are defined by substituting the natural and spike isotopic ratios into this equation. For Eq. (12):

$$x = \frac{^{180}Hf/^{177}Hf_{spike} - {}^{180}Hf/^{177}Hf_{natural}}{^{179}Hf/^{177}Hf_{spike} - {}^{179}Hf/^{177}Hf_{natural}}, \quad \text{and}$$

$$y = {}^{180}Hf/^{177}Hf_{spike} - x \times {}^{179}Hf/^{177}Hf_{spike}.$$

In these equations, the ratios used are the 'true' natural and spike ratios based on $^{179}Hf/^{177}Hf_{natural} = 0.7325$. In reality, a constant and consistent set of ratios is acceptable.

These equations can be simply recast to a single equation in *R*:

$$\frac{^{180}(Hf + W + Ta)}{^{177}Hf} - \frac{^{181}Ta}{^{177}Hf} \times \frac{^{180}Ta}{^{181}Ta} \times R^b - \frac{^{182}W}{^{177}Hf} \times \frac{^{180}W}{^{182}W} \times R^c - \Phi^{-1} \times \left(x \times R \times \frac{^{179}Hf}{^{177}Hf} + y\right) \times R^{-a} = 0 \quad (14)$$

In the analysis spreadsheet, an initial estimate of *R* is made from observed $^{179}Hf/^{177}Hf$ in a nearby standard. Based on this, the value of the expression in Eq. (14) is evaluated for each integration, and a new estimate of *R* is made for each integration until the expression is <0.0000005. A new estimate of *R* is conveniently generated by multiplying the previous *R* estimate by $(1-z{\cdot}Q)$, where *Q* is the evaluated expression of Eq. (14) and *z* is a single constant that controls

the rate of convergence to zero for all integrations. The value of R so determined for each integration is then used to adjust natural isotope ratios such as $^{176}Yb/^{172}Yb$ for sample mass bias and thus allow interference corrections to all Hf isotope ratios. R is also used to mass bias correct all Hf isotope ratios. Finally, the Hf isotope ratios are corrected for the spike contribution.

For static Nd, the system is more complicated because the Sm correction appears in the expression for R, and also because any real Sm in the sample will have non-natural Sm ratios due to a component of Sm spike. But the same principles can be used to derive an equation analogous to (14) which is iterated to generate $R = (^{146}Nd/^{144}Nd_{N,\,Sm})/(^{146}Nd/^{144}Nd_{Sm})$, where subscript Sm implies Sm-corrected:

$$\Phi \times {}^{150}Nd/{}^{144}Nd \times R^a \times \frac{1 - {}^{147}Sm/{}^{150}Nd \times \Phi^{-1} \times R^{-d} \times (y \times R^b \times {}^{149}Sm/{}^{147}Sm + z)}{1 - {}^{147}Sm/{}^{144}Nd \times R^{-c} \times (w \times R^b \times {}^{149}Sm/{}^{147}Sm + x)} - v - u \times \frac{{}^{146}Nd/{}^{144}Nd \times R}{1 - {}^{147}Sm/{}^{144}Nd \times R^{-c} \times (w \times R^b \times {}^{149}Sm/{}^{147}Sm + x)} = 0 \quad (15)$$

where all isotope ratios used are uncorrected for interference or mass bias, and u, v, w, x, y, z are defined by substituting natural and spike ratios into the following spike:natural mixing equations:

$$\left(\frac{^{150}Nd}{^{144}Nd}\right)_{N,\,Sm} = u \times \left(\frac{^{146}Nd}{^{144}Nd}\right)_{N,\,Sm} + v$$

$$\left(\frac{^{144}Sm}{^{147}Sm}\right)_{N,\,Nd} = w \times \left(\frac{^{149}Sm}{^{147}Sm}\right)_{N} + x$$

$$\left(\frac{^{150}Sm}{^{147}Sm}\right)_{N,\,Nd} = y \times \left(\frac{^{149}Sm}{^{147}Sm}\right)_{N} + z$$

and a, b, c, d are mass coefficients $a = \ln(M_{150}/M_{144})/\ln(M_{146}/M_{144})$, b=$\ln(M_{149}/M_{147})/\ln(M_{146}/M_{144})$, $c = \ln(M_{144}/M_{147})/\ln(M_{146}/M_{144})$ and $d = \ln(M_{150}/M_{147})/\ln(M_{146}/M_{144})$.

The processing of multidynamic ID samples is more complex because the multidynamic algorithms use peak intensities instead of ratios. The exponential-law multidynamic expression for $^{180}Hf/^{177}Hf_N$ (Eqs. (1) and (7)) requires W and Ta corrected intensities 180_2 and 180_3, so Eqs. (12) and (13) from the static calculation must be combined with:

$$\left(\frac{^{180}Hf}{^{177}Hf}\right)_T = \Phi \times \left(\frac{^{179}Hf}{^{177}Hf}\right)_N \times \left(\frac{180_2 \times 180_3 \times 177_1 \times (^{179}Hf/^{177}Hf)_N}{179_1 \times 179_2 \times 179_3}\right)^{0.5} \times R^{(a-1.5)} \quad (16)$$

$$180_2 = {}^{180}(Hf + W + Ta)_2 - \left(\frac{^{181}Ta}{^{177}Hf}\right)_3 \times {}^{177}Hf_2 \times \frac{^{180}Ta}{^{181}Ta} \times R^b - {}^{182}W_2 \times \frac{^{180}W}{^{182}W} \times R^c \quad (17)$$

$$180_3 = {}^{180}(Hf + W + Ta)_3 - {}^{181}Ta_3 \times \frac{^{180}Ta}{^{181}Ta} \times R^b - \left(\frac{^{182}W}{^{177}Hf}\right)_2 \times {}^{177}Hf_3 \times \frac{^{180}W}{^{182}W} \times R^c \quad (18)$$

to derive an equation containing just R, with 180_2 and 180_3 defined by Eqs. (17) and (18):

$$\Phi \times \frac{^{179}Hf}{^{177}Hf} \times R \left(\frac{180_2 \times 180_3 \times 177_1 \times {}^{179}Hf/{}^{177}Hf \times R}{179_1 \times 179_2 \times 179_3}\right)^{0.5} \times R^{(a-1.5)} - x \times R \times \frac{^{179}Hf}{^{177}Hf} - y = 0 \quad (19)$$

where Φ, R, a, b, c, x and y are defined as for static Hf.

This expression is iterated in the same way as described above for spiked static runs. It might be considered that this expression is not truly multidynamic, since the static $^{179}Hf/^{177}Hf$ appears in it three times. However, in each it is multiplied by R, thus yielding $^{179}Hf/^{177}Hf_N$ which is not static dependent. The value of R does however contain inaccuracies resulting from the static $^{179}Hf/^{177}Hf$, but these only appear in the interference corrections (Eqs. (17) and (18)) and in the conversion from power to exponential normalisation (the $R^{(a-1.5)}$ term of Eq. (16)). In both cases likely static uncertainties have insignificant impact, as shown above for unspiked multidynamic data.

Yb interference on ^{176}Hf can be accurately corrected for samples spiked with our mixed REE spike, which is enriched in ^{171}Yb and ^{176}Lu, in combination with a ^{180}Hf spike. In multidynamic runs, $^{173}Yb/^{171}Yb$ is measured in jump 1, and can be corrected for mass bias once R is known. Through the natural-spike mixing equation, the normalized $^{176}Yb/^{172}Yb$ in the mixture can be calculated. In static runs this is not possible, but inaccurate values for $^{174}Hf/^{177}Hf$ can be used as an indicator that a problem exists with the Yb correction. Since $^{176}Yb/^{174}Yb \approx 0.4$, a Yb-induced inaccuracy in $^{174}Hf/^{177}Hf$ at the 0.000005 limit of the external precision would only result in inaccuracy of 0.000002 in $^{176}Hf/^{177}Hf$, insignificant compared to the internal precision. Although non-natural Yb in the Hf analysis can be rigorously corrected, the existence of only two Lu isotopes means that ^{176}Lu spike in a Hf run cannot be accurately corrected. The $^{176}Lu/^{175}Lu$ of Lu in the Hf analysis must however lie between the natural ratio (0.02645, which would imply that all Lu in the Hf run was blank) and the ratio in the spiked sample, which is itself measured independently to derive the Lu concentration. It must also be less than $^{176}Lu/^{175}Lu$ in the

spike (∼2.5). The best practice is to propagate uncertainty in $^{176}Lu/^{175}Lu$ in the Hf analysis into the $^{176}Hf/^{177}Hf$ error.

4. Results

4.1. TIMS Yb and Nd data

Tables 3 and 4 report results of our multidynamic TIMS analyses of Aldrich Yb and Nd solutions. The Yb data, which were determined over two years, lie within error of the TIMS ratios of [17], but with 5–8× better external precision (Table 3). Each individual analysis in our mean is the mean of 60–80 scans using 5 s integration times with an ion beam of $\sim 2 \times 10^{-11}$ A ^{174}Yb. Because equivalent information is not provided by [17], we cannot identify whether better counting statistics or the use of multidynamic data is the cause of the improved reproducibility.

We report four sets of multidynamic TIMS data for the Aldrich Nd standard in Table 4, in which each analysis represents the mean of ∼105 scans with $2–3 \times 10^{-11}$ A ^{144}Nd using 5 s integration times. All data sets show good correlations between $^{146}Nd/^{144}Nd$ and power-law-normalized ratios, which are eliminated by exponential normalisation. The first set used our usual collector configuration [9] for a 6 month period following the installation of long-life Faraday buckets in 1994. Peaks were centred in the axial Faraday (Table 1) which optimises measurement of $^{142}Nd/^{144}Nd$, $^{143}Nd/^{144}Nd$ and $^{145}Nd/^{144}Nd$, as it minimises the inevitable misalignment of peak flats in jumps 1 and 3 in an instrument without zoom optics. The other data sets used four separate loads of the Aldrich standard, two of a JMC Nd, and one of JNdi-1 [21], each repeatedly analysed using the TIMS1 and TIMS2 collector set-ups (Table 1). TIMS1 is comparable to the routine set-up, while TIMS2 is instead optimised for measurement of $^{148}Nd/^{144}Nd$ and $^{150}Nd/^{144}Nd$ by centring on the H1 Faraday. The effects of non-optimised peak centring can clearly be seen in higher $^{148}Nd/^{144}Nd$ using TIMS1 and higher $^{142}Nd/^{144}Nd$ and $^{143}Nd/^{144}Nd$ using TIMS2 (Table 4). The apparent overlap in reported uncertainties is a consequence of these being external precision: the mean values are significantly different because the N multiple analyses give additional confidence in the mean by a factor of $N^{-0.5}$. Some beads were also run using TIMS2 but using centring on L1 so as to mimic TIMS1 (Table 1). These yield Nd ratios identical to those using TIMS1, demonstrating that our reported ratios are independent of collectors used.

In Table 4 our measured Nd ratios are compared with the non-radiogenic Nd ratios of [7,22], which surprisingly appear to be the only complete non-radiogenic Nd TIMS data in the literature. The former were measured in single collector mode on NdO^+ ion beams using normalisation to $^{146}Nd/^{142}Nd = 0.636151$, and, despite expressing the view that the exponential law best expressed TIMS Nd fractionation, Wasserburg et al. [7] used the power law to renormalize to $^{146}Nd/^{144}Nd = 0.7219$. There are substantial differences between the power and exponential-law renormalized values (Table 4; [9]). Further, their Nd isotope ratios have *after renormalization* a moderately strong dependence on the assumed oxygen isotope ratios. Wasserburg et al. [7] changed their previously assumed oxygen ratios to values actually measured on their mass spectrometer, and in Table 4 we have estimated uncertainties on their ratios based on their reported spread in measured oxygen ratios. Thus, there may be systematic error from the assumed oxygen composition. Caro et al. [22] used a Finnegan Triton in static mode to generate very high precision data for the AMES standard and rock samples, but no details were given of the methods used to calibrate collector efficiencies, and thus the data may not be accurate. Apart from $^{150}Nd/^{144}Nd$, our data (Table 4) are within error of the exponential-law-renormalized ratios of [7], but both our $^{142}Nd/^{144}Nd$ and $^{150}Nd/^{144}Nd$ are substantially higher than the values of [22]. At present we see no reason not to accept our new TIMS values for comparison with IsoProbe data since identical multidynamic calculations are used.

4.2. Results of static analyses of JMC475 Hf solution

As with Nd [5], raw static Hf ratios show very good correlations ($r^2 > 0.998$) with each other on ln(ratio) plots, with gradients comparable to but not entirely within error of expected exponential-law gradients (Table 5). There is substantial scatter on these correlations outside analytical error as indicated by MSWD values from 3.4 to 27.3.

Reproducibility of normalized static $^{174}Hf/^{177}Hf$ is excellent at only 2.6× mean internal precision, based on 113 analyses over 2.3 years (Table 6). Static $^{180}Hf/^{177}Hf$ and $^{178}Hf/^{177}Hf$ data show reproducibility comparable to that reported by many other laboratories (Table 6), but our reproducibility of static $^{176}Hf/^{177}Hf$ (±0.000053 or 200 ppm 2S.D.) is rather worse than reported by most other MC–ICP–MS laboratories. External precision of these ratios is ∼10× average internal precision, requiring other error sources to be much greater than counting statistics. Apart from $^{174}Hf/^{177}Hf$, normalized static ratios show substantial variation with time (Fig. 2), both at the scale of months and occasionally on single days (e.g. the last session in 8/01 and the first in 4/02). The time variation is cyclic rather than unidirectional, though there are long periods of unidirectional change apparent (Fig. 2). We can deal with the temporal variation by frequent measurement of JMC475 standard, as advocated by [2,4]. Of 13 analytical sessions when more than 3 standards were analysed, 9 have session external precision better than 50 ppm 2S.D., and the rest have session external precision better than 85 ppm 2S.D., comparable values to those reported by other laboratories (Table 6). This effectively limits sample precision to ∼50 ppm, or worse when there is large drift in a single day e.g. the last session

Table 5
Regression parameters for ln(ratio)–ln(ratio) plots of IsoProbe data, using static ratios from multidynamic runs uncorrected for mass bias.

	$^{174}Hf/^{177}Hf^a$	$^{176}Hf/^{177}Hf^a$	$^{178}Hf/^{177}Hf^a$	$^{180}Hf/^{177}Hf^a$	N	$^{142}Nd/^{144}Nd^a$	$^{143}Nd/^{144}Nd^a$	$^{145}Nd/^{144}Nd^a$	$^{150}Nd/^{144}Nd^a$	N
	$^{179}Hf/^{177}Hf^b$	$^{179}Hf/^{177}Hf^b$	$^{179}Hf/^{177}Hf^b$	$^{179}Hf/^{177}Hf^b$		$^{146}Nd/^{144}Nd^b$	$^{146}Nd/^{144}Nd^b$	$^{146}Nd/^{144}Nd^b$	$^{146}Nd/^{144}Nd^b$	
Gradient (all runs)	−1.519 ± 0.021	−0.507 ± 0.002	0.496 ± 0.002	1.497 ± 0.003	88	−0.981 ± 0.010	−0.476 ± 0.007	0.515 ± 0.003	2.997 ± 0.011	64
MSWD	3.4	14.5	27.3	7.9		96	121	15	20	
Gradient*	–	−0.500 ± 0.007	0.507 ± 0.005	1.505 ± 0.006	11	−1.05 ± 0.03	−0.520 ± 0.011	0.520 ± 0.010	3.02 ± 0.04	29
MSWD	–	3.1	2.4	1.0		13	5.7	4.0	8.5	
Expected gradients										
Exponential law	−1.521	−0.5045	0.5010	1.4956		−1.014	−0.505	0.502	2.960	
Power law	−1.500	−0.5003	0.4996	1.4998		−1.000	−0.499	0.500	3.001	
GPL $q = -0.6$	−1.534	−0.507	0.5019	1.4931		−1.022	−0.508	0.503	2.936	

Gradients calculated using Isoplot [27]; those indicated by * were for September 2003 (Hf) and pre-upgrade data (Nd). Uncertainties (at 95% confidence) are derived from ratio internal precision multiplied by $\sqrt{\text{MSWD}}$. GPL, general power law [6,20] with exponent $q = -0.6$.
[a] y-axis.
[b] x-axis.

in 8/01. The variation in $^{178}Hf/^{177}Hf$ and $^{180}Hf/^{177}Hf$ is less (∼100 ppm), but the latter at least should be corrected for isotope dilution samples to avoid additional error propagation to Hf contents, as samples are usually underspiked to minimise spike correction to $^{176}Hf/^{177}Hf$. For example, a sample underspiked to give $^{180}Hf/^{177}Hf = 1.95$ could have ∼1% systematic error on Hf contents if a natural ratio incorrect by 0.02% was assumed. Any such correction presumes that the drift operates identically for samples as for standards, and the errors on standard and sample runs, together with the error in estimating any drift, should be propagated into the final sample error. Because of these problems we chose to investigate multidynamic analysis.

4.3. Results of multidynamic IsoProbe analyses

4.3.1. Hf

Fig. 3 and Table 6 report results of 88 multidynamic analyses of JMC475 standard over a 2.8 year period. $^{174}Hf/^{177}Hf$ cannot be calculated via a multidynamic algorithm with our current jumping sequence and thus static data from the multidynamic runs are presented, which agree well with true static results. Two static calculations are possible in multidynamic runs, using data from jump 1 or jump 2, the latter being reported in Table 6. External precision on $^{174}Hf/^{177}Hf$ using jump 2 is 2× average internal precision, while external precision on data from jump 1 is much worse, at 4.5×. This is true whether or not we make a simultaneous correction for Yb interference in jump 1. External precision on static $^{176}Hf/^{177}Hf$ is also worse on jump 1 than jump 2, but the excess variation in the two ratios is not correlated, so it is not caused by Yb correction problems.

Multidynamic $^{176}Hf/^{177}Hf$ has significantly better external reproducibility than static $^{176}Hf/^{177}Hf$ from the multidynamic runs (66 ppm 2S.D. compared with 105 ppm, Fig. 3), little worse than the best static data from other laboratories (Table 6), which were in the main accumulated over a much shorter time period. The improvement in external precision may in part reflect the better internal precision of the multidynamic run due to integration of more ^{176}Hf ions per analysis (seen in mean internal precision improving from 23 to 17 ppm 2S.E.), but this cannot be the main cause of the improved multidynamic performance, given that external precision is in both cases much worse than internal.

Multidynamic $^{178}Hf/^{177}Hf$ and $^{180}Hf/^{177}Hf$ also show much better external precision than static ratios from the same run (60 and 75 ppm 2S.D., respectively multidynamic, compared with 115 and 154 ppm static, Fig. 3). Our multidynamic $^{180}Hf/^{177}Hf$ data in particular is comparable to the best static data from other laboratories. The multidynamic ratios show much less secular variation, particularly during 2001, before a major change to the interface as part of an instrument upgrade. At times both these static ratios are much lower (late 2001) or much higher (January 2001) than the

Table 6
Hf isotope ratios from Royal Holloway and literature sources

	$^{174}Hf/^{177}Hf$	$^{176}Hf/^{177}Hf$	$^{178}Hf/^{177}Hf$	$^{180}Hf/^{177}Hf$	*N*
Royal Holloway IsoProbe					
Static, >30 pA ^{180}Hf	0.008657 ± 05	0.282190 ± 53	1.46735 ± 16	1.88669 ± 21	58–113
Multidynamic	–	0.282165 ± 18	1.46733 ± 09	1.88686 ± 14	88
Multidynamic, corrected to const. $^{178}Hf/^{177}Hf$		0.282165 ± 14			
Mean internal precision		0.000005	0.000013	0.000028	
Static on multidynamic run	0.008659 ± 05	0.282181 ± 30	1.46734 ± 17	1.88676 ± 29	88
Mean internal precision	0.000002	0.000007	0.000018	0.000036	
Literature data					
Multidynamic TIMS [30]	–	0.282157 ± 89	1.46717 ± 14	1.88667 ± 30	55
P54 [16]	–	0.282163 ± 09	1.46717	1.88667	29
P54 [24], static, same lab as [16]	–	0.282154 ± 28	–	–	23
P54, one session? [29]	0.008647 ± 20	0.282162 ± 14	1.46749 ± 07	1.88747 ± 37	?
TIMS [32]	–	0.282165 ± 93	1.46717 ± 10	1.88679 ± 29	24
IsoProbe, AMES Hf [33]	–	0.282151 ± 13	1.46718	1.88652	?
IsoProbe [17]	0.008674 ± 32	0.282163 ± 26	1.46742 ± 23	1.88677 ± 29	79
Nu Plasma [17]	–	0.282159 ± 38	1.46730 ± 15	1.88668 ± 63	20
Nu Plasma [23]	–	0.282161 ± 34*	1.46727 ± 04	1.88677 ± 20	208
Nu Plasma [28]	–	0.282169 ± 16	1.46729 ± 08	1.88680 ± 30	?
VG Axiom, not JMC475 [34]	–	0.281878 ± 15	1.46719 ± 04	1.88670 ± 10	54

Uncertainties are 2S.D. where given; for [30] 2S.D. was recalculated from 2S.E. values originally reported (P.J. Patchett, personal communication., 2003). *N*, no. of analyses in mean. All samples JMC475 and all static except where stated. All data normalized to $^{179}Hf/^{177}Hf = 0.7325$ using exponential law. [16]: $^{176}Hf/^{177}Hf$ multidynamic, other ratios static, possibly with cup efficiencies adjusted to give the same ratios as [30]. (*) from [35], $N = 40$.

multidynamic results; at other times they are broadly similar (e.g. September 2003); while at other times one static ratio may be similar to the multidynamic value and one very different (e.g. September 2002). The multidynamic data does however also show secular variation, with for example high values of all ratios around April 2002, and low values in September 2003. This implies at least two separate causes for secular variation, one affecting static data alone and one both static and multidynamic. After the instrument upgrade in March 2002, we have observed that the instrument in general gives higher multidynamic Hf isotope ratios in soft than in hard extraction mode. This is particularly clear in the data from September 2003, where data were obtained in alternating soft and hard extraction mode. However, the optimum

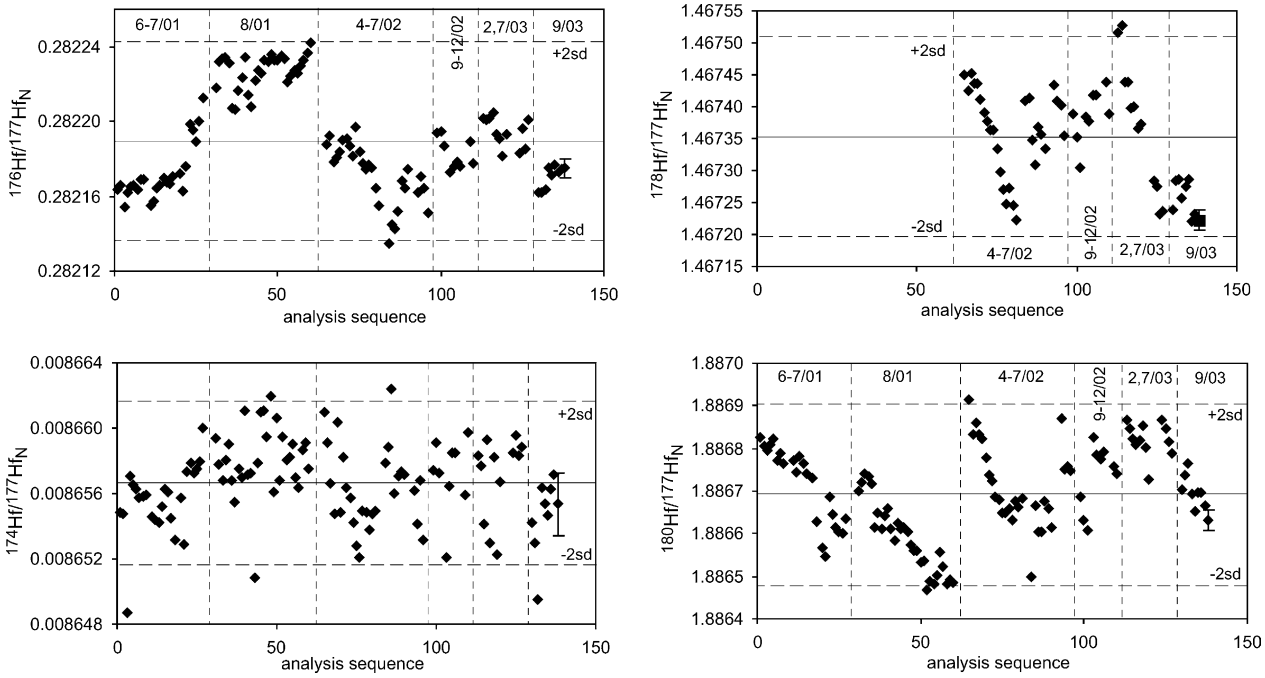

Fig. 2. Results of normal static IsoProbe analyses of JMC475 Hf solution between June 2001 and September 2003. Error bar represents mean internal precision (2S.E.) of the analyses, horizontal lines mean and 2S.D. of the dataset.

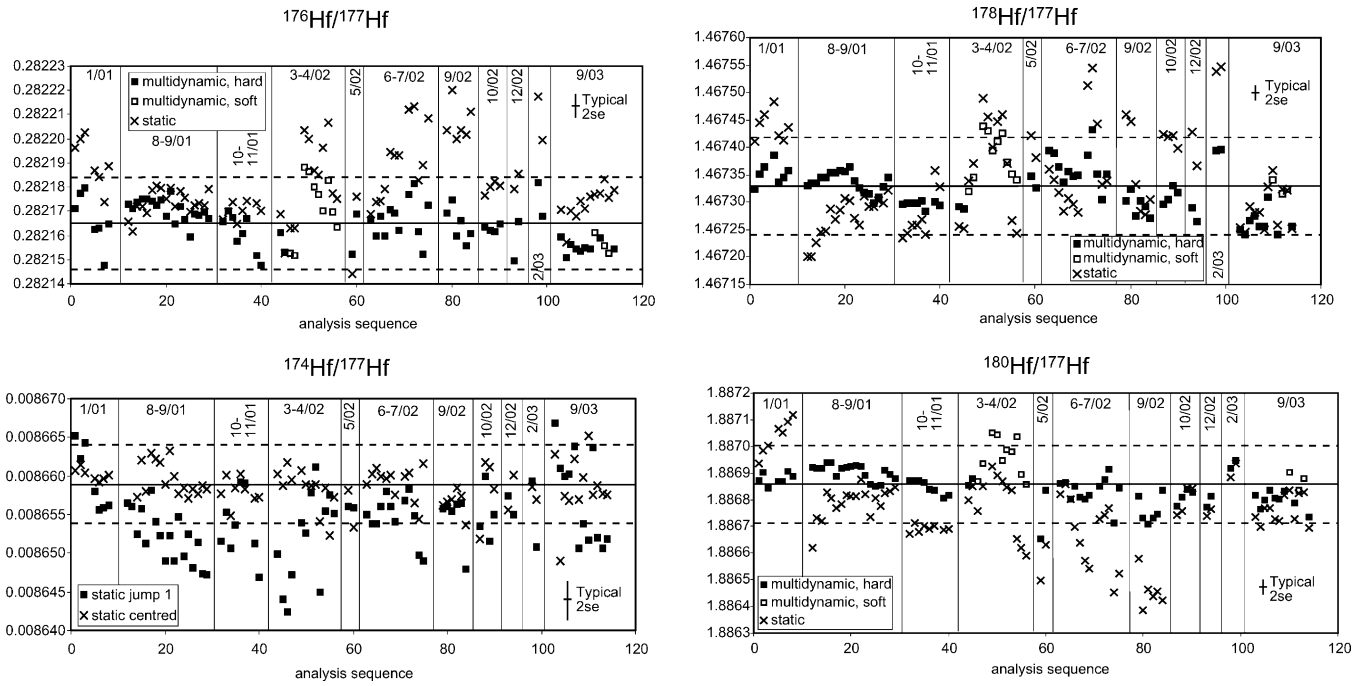

Fig. 3. Results of multidynamic IsoProbe analyses of JMC475 Hf solution between January 2001 and September 2003. All static data plotted are static results calculated from the multidynamic runs (i.e. not the same runs as Fig. 2). "Hard" and "soft" signify hard and soft extraction mode. Error bar represents mean internal precision (2S.E.) of the analyses, horizontal lines mean and 2S.D. of the multidynamic dataset (except only a static calculation is possible for $^{174}Hf/^{177}Hf$).

extraction potential is lower in soft than hard extraction, and reducing hard extraction potential also appears to increase multidynamic Hf ratios since the upgrade (Fig. 4).

The multidynamic ratios show broad positive correlations with each other (Fig. 5). In some time periods (e.g. 3–4/02, 5–9/02, 9/03) these correlations are in part defined by changes in extract potential. $^{176}Hf/^{177}Hf$ and $^{178}Hf/^{177}Hf$ show a single correlation for all time periods, while data for 5–9/02 are offset to lower $^{180}Hf/^{177}Hf$ than other time periods on diagrams involving $^{180}Hf/^{177}Hf$. Regression results from these correlations are given in Table 7, excluding data from 5/02 to 9/02 for regressions involving $^{180}Hf/^{177}Hf$. Despite scatter substantially outside internal precision on the ratios, these correlations all have gradients within error of 1.0 on ln–ln plots. There are also rough correlations between normalized multidynamic ratios and the measured $^{179}Hf/^{177}Hf$ (e.g. Fig. 4): these show strong time-related groupings, with an offset to lower $^{179}Hf/^{177}Hf$ being evident for data collected after the upgrade of March 2002.

4.3.2. Nd

Table 4 and Fig. 6 report results of 64 multidynamic IsoProbe analyses of our Aldrich standard. Multidynamic ratios determined prior to the upgrade (four measurement

Table 7
Regression parameters for multidynamic Hf and Nd isotope ratios

	$^{176}Hf/^{177}Hf$[a] $^{178}Hf/^{177}Hf$[b]	$^{176}Hf/^{177}Hf$[a] $^{180}Hf/^{177}Hf$[b]	$^{180}Hf/^{177}Hf$[a] $^{178}Hf/^{177}Hf$[b]	$^{143}Nd/^{144}Nd$[a] $^{142}Nd/^{144}Nd$[b]	$^{145}Nd/^{144}Nd$[a] $^{142}Nd/^{144}Nd$[b]	$^{150}Nd/^{144}Nd$[a] $^{142}Nd/^{144}Nd$[b]
Gradient	0.15 ± 0.04	0.14 ± 0.03	1.32 ± 0.19	0.29 ± 0.02	0.09 ± 0.02	0.25 ± 0.03
MSWD	8.3	5.1	4.8	8.1	26	14
Gradient*	0.80 ± 0.18	0.96 ± 0.18	1.03 ± 0.15	0.64 ± 0.05	0.29 ± 0.06	1.23 ± 0.15
Expected*	–3.04 ± 0.08	1.02 ± 0.05	–2.96 ± 0.07	0.372 ± 0.006	–0.122 ± 0.006	2.96 ± 0.09
TIMS*	–	–	–	0.39	–0.15	–

Gradients calculated using Isoplot [27]; uncertainties (2s) are derived from ratio internal precision multiplied by $\sqrt{\text{MSWD}}$. (*) gradients for ln(ratio)–ln(ratio) plots. Expected = correlation gradients expected on ln(ratio)–ln(ratio) plots if mass bias really followed the general power law (with exponent q ranging from +5 to −5), but the data were actually corrected using exponential law. Uncertainties given for these are 2S.D. on gradients calculated for integer q between +5 and −5, with $q = 0$ replaced by $q = 0.0001$. TIMS*, TIMS gradients reported by [9] for power-law-corrected ratios, recast to gradients on ln–ln plots.

[a] y-axis.
[b] x-axis.

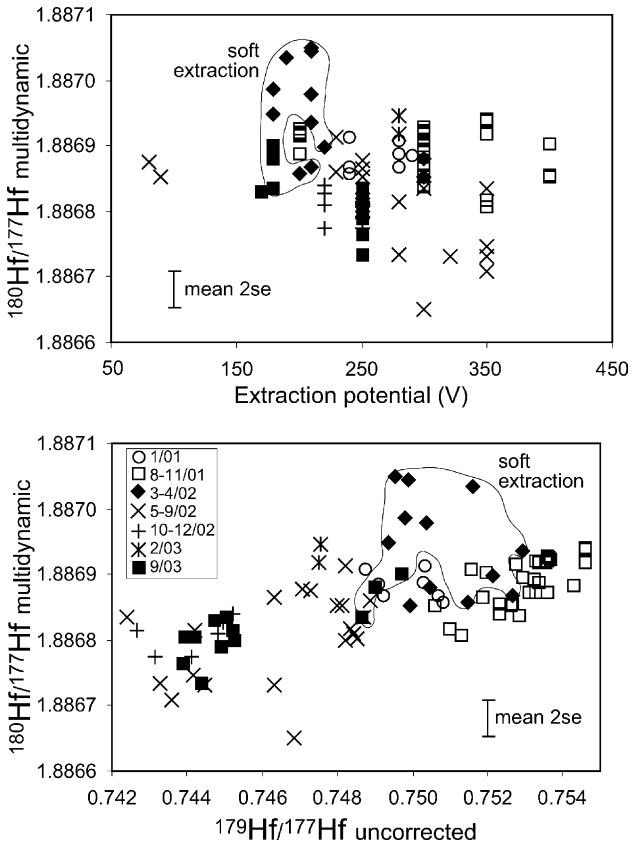

Fig. 4. The effect of extraction potential and mean mass bias, represented by $^{179}Hf/^{177}Hf$, on multidynamic IsoProbe analyses of JMC475 Hf solution between January 2001 and September 2003. Error bar represents mean internal precision (2S.E.) of the analyses. Symbols represent analyses obtained in different time periods of Fig. 3. The soft extraction field shows soft extraction measurements from April 2002 and September 2003. Data acquired since the interface upgrade in early 2002 show a broad correlation between multidynamic $^{180}Hf/^{177}Hf$ and extract potential, and a correlation with $^{179}Hf/^{177}Hf$ offset to slightly higher $^{180}Hf/^{177}Hf$ than that of pre-upgrade data.

sessions), and in soft extraction since (nine measurement sessions), are reproducible to 30–90 ppm 2S.D., only 2–3× worse than the mean internal precision (Table 4) and comparable to the 60–75 ppm external precision for multidynamic Hf ratios. Static ratios measured on the same runs are only reproducible to 60–350 ppm, though as with Hf, static reproducibility is good within single analytical sessions of a few days. In contrast, multidynamic data from hard extraction runs since the upgrade (11 measurement sessions) have 108–414 ppm 2S.D. external precision, not much better than the 140–470 ppm of static data from the same runs. There are good correlations (Fig. 6) between all multidynamic ratios except $^{148}Nd/^{144}Nd$, with gradients against $^{142}Nd/^{144}Nd$ given in Table 7. There is considerable scatter on all correlations outside analytical error, as illustrated by MSWDs from 8 to 26 (Table 7). The correlations, and the scatter, are primarily defined by the post-upgrade hard extraction data: pre-upgrade data have a $^{143}Nd/^{144}Nd$-$^{142}Nd/^{144}Nd$ correlation with MSWD < 1.

Fig. 6 also shows the TIMS Nd ratios for comparison. As observed by [5], apart from $^{145}Nd/^{144}Nd$ in the pre-upgrade and soft extraction data, all multidynamic IsoProbe ratios are lower than the equivalent TIMS ratios. However, in this study the correlations do not intersect the TIMS ratios, perhaps because the wider spread in $^{142}Nd/^{144}Nd$ allows better definition of the slopes. Accordingly, if we use the empirical correction method proposed by [5,9], we generate corrected $^{143}Nd/^{144}Nd$ ratios much higher than the TIMS value. The reproducibility of our pre-upgrade and soft extraction data is intermediate between those of the two published MC–ICP–MS Nd data sets, while our hard extraction data set is substantially worse.

4.3.3. Yb

The results of six multidynamic Yb analyses on the IsoProbe are given in Table 3. These were all measured in soft extraction on a single day and thus reproducibility of multidynamic ratios and of static ratios on the multidynamic runs is very similar, and very similar to the mean internal precision. Static data collected over a 1.5 year period shows 2S.D. external reproducibility around 75 ppm (Table 3), as might be expected through comparison with Hf. Apart from $^{173}Yb/^{172}Yb$, the multidynamic IsoProbe ratios are lower than the equivalent TIMS ratios, as seen for Nd.

4.3.4. Pb

Thirlwall [8] showed that static $^{204}Pb/^{206}Pb$ and $^{207}Pb/^{206}Pb$ on the IsoProbe normalized to constant $^{208}Pb/^{206}Pb$ had external precision of ∼100 ppm 2S.D., little worse than internal precision, over the year ending March 2001. Reproducibility of static $^{207}Pb/^{206}Pb$ has worsened substantially since (Fig. 7), and a multidynamic Pb routine was introduced based on [25]. Normalisation was either to the known $^{208}Pb/^{206}Pb$ (standards), or to the mean static $^{208}Pb/^{206}Pb$ (unknowns). The internally-normalized multidynamic $^{207}Pb/^{206}Pb$ data of SRM981 are very similar to the static data of [8], and have 2.5× better external precision than contemporaneous static runs, or static ratios calculated from multidynamic runs (Fig. 7, Table 8). The large changes in static $^{207}Pb/^{206}Pb$ in 2001–2002 caused problems in applying mass bias corrections using the ^{207}Pb–^{204}Pb double spike (DS, [8]), because the errors are propagated into all the Pb ratios. Offsets of up to 200 ppm were observed in all ratios with external precision worsening by a factor of 2. We therefore recalibrated the double spike using multidynamic runs of the pure spike and SRM982, which resulted in spike isotope ratios almost indistinguishable from those reported in [8]. Fourteen multidynamic analyses of SRM981 and SRM981–DS mixtures (Table 8) yielded external precision almost identical to the propagated internal precision on the DS-corrected ratios, and ratios for mass-bias-corrected SRM981 very similar to those reported by [8].

Analysis of Pb by multidynamic techniques unfortunately imposes a major penalty on the measurement of $^{204}Pb/^{206}Pb$, as the low-intensity ^{204}Pb can only be

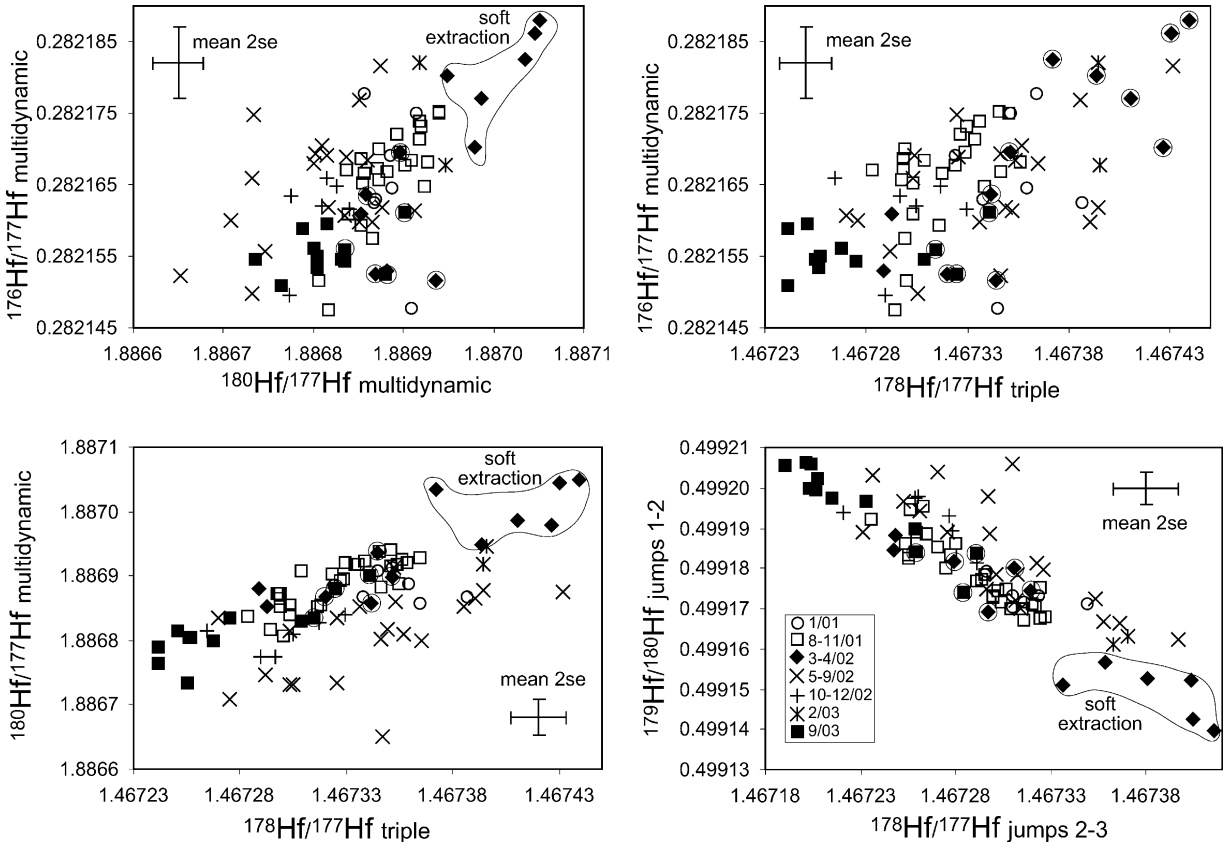

Fig. 5. Results of multidynamic IsoProbe analyses of JMC475 Hf solution between January 2001 and September 2003. Error bar represents mean internal precision (2S.E.) of the analyses. Symbols represent analyses obtained in different time periods of Fig. 3, those enclosed by circles, together with the field outlined, are soft extraction data.

measured once per cycle (see [25] for collector alignment). However, two independent static measurements of $^{204}Pb/^{206}Pb$ can be made in jumps 2 and 3, in addition to the dynamic measurement which uses ^{204}Pb measured in jump 1. These two static measurements have similar external precision to the dynamic measurement (Table 8), because the ~100 ppm uncertainty imposed by the counting statistics on small ^{204}Pb ion beams is comparable to that imposed by the static mode on $^{207}Pb/^{206}Pb$. Consequently, a geometric mean of these three $^{204}Pb/^{206}Pb$ measurements can be used for natural samples with low $^{204}Pb/^{206}Pb$. Static mode errors however mean that the dynamic $^{204}Pb/^{206}Pb$ analysis alone must be used for DS-sample mixtures, but as $^{204}Pb/^{206}Pb$ is high in such samples, it is possible to get adequate precision from a much smaller number of ratios.

Table 8
Multidynamic Pb data for SRM981 and SRM982

	$^{204}Pb/^{206}Pb$	$^{207}Pb/^{206}Pb$	$^{208}Pb/^{206}Pb$	*N*
Internal normalisation to constant $^{208}Pb/^{206}Pb$				
SRM981	0.059022 ± 09	0.914892 ± 031	*2.1677*	27
Mean 2S.E.	0.000003	0.000013		
Static on multi runs jump 2	0.059018 ± 08	0.914819 ± 082	*2.1677*	27
Static on multi runs jump 1	0.059013 ± 06	0.914889 ± 107	*2.1677*	27
SRM982	0.027207 ± 04	0.467090 ± 007	*1.00016*	3
Mass bias correction using double spike				
SRM981–DS multidynamic	0.059021 ± 07	0.914888 ± 040	2.16768 ± 12	14
Mean 2S.E.	0.000005	0.000036	0.00017	
SRM981–DS static [8]	0.059026 ± 10	0.914880 ± 080	2.16770 ± 24	36

Errors quoted are 2S.D.: *N*, no. of analyses in mean. Mean 2S.E. for double-spike-corrected multidynamic data is internal precision propagated through the correction algorithm: this over-estimates error somewhat since minor in-run mass bias variability contributes to the internal precision but is corrected by the double spike correction.

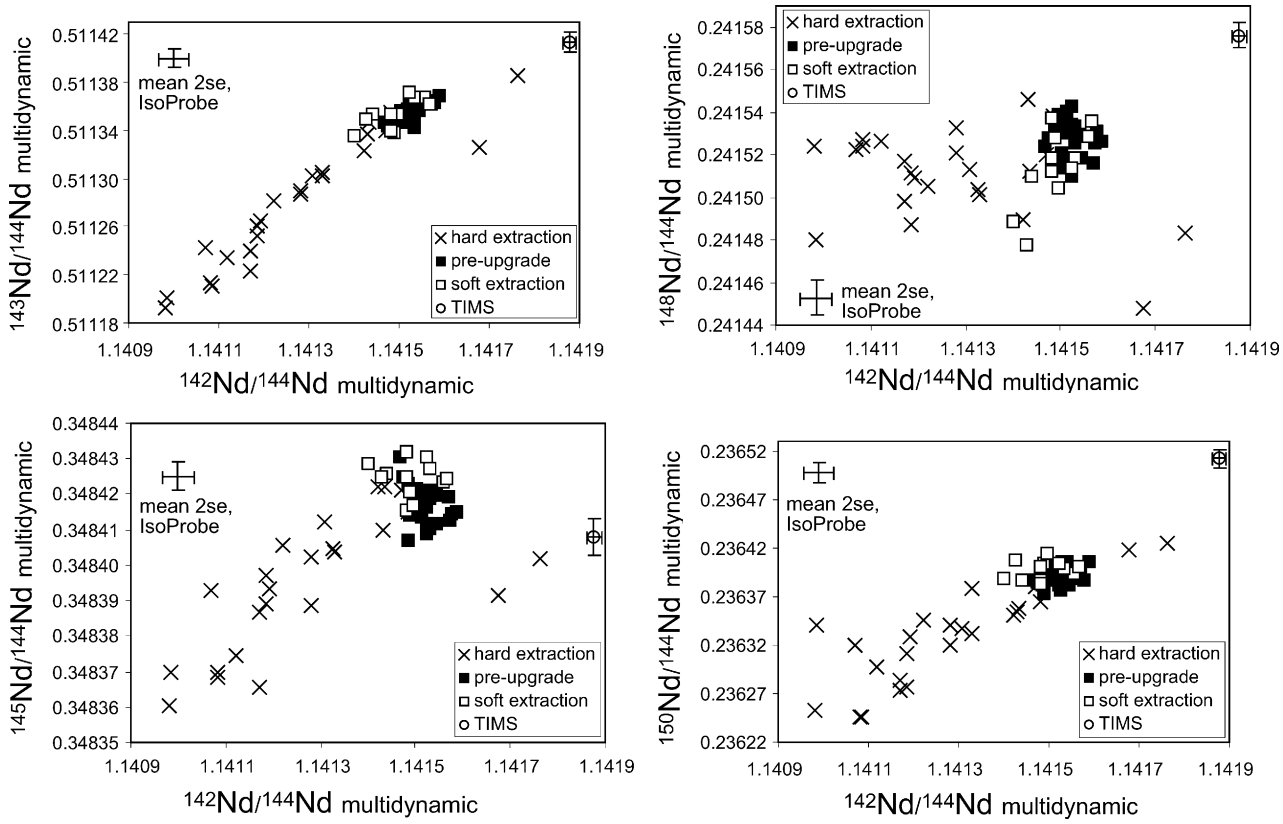

Fig. 6. Results of multidynamic IsoProbe analyses of Aldrich Nd solution between September 2001 and October 2003, compared with TIMS data from Table 4. Error bar represents mean internal precision (2S.E.) of the analyses, and 2S.D. external precision for the TIMS analyses.

4.4. Results of isotope dilution analyses

The spiked Hf and Nd runs yield several corrected non-radiogenic ratios for all samples. These provide tests of the corrections for spike, mass bias and Yb, Ce or Sm interferences in real chemically-separated samples, because they should be within error of the same ratios determined on unspiked samples on the same day. Further, the R value defined by Eq. (13) should be similar to that calculated from nearby unspiked samples. The success of the equations derived above is illustrated in Fig. 8, where static Hf data, and both multidynamic and static Nd data, on a wide variety of rock and mineral types, are compared with standard data. Sample data for $^{174}Hf/^{177}Hf$, which is strongly affected by the accuracy of the Yb correction, are entirely within error of the standard data. There is a slight tendency for sample $^{178}Hf/^{177}Hf$ data to be higher than contemporaneous standard data (Fig. 8), and there is a rough correlation between $^{178}Hf/^{177}Hf$ and the sample $^{180}Hf/^{177}Hf$. This suggests a minor problem with the spike correction, which is biggest on $^{178}Hf/^{177}Hf$, although the spike $^{178}Hf/^{177}Hf$ needed to eliminate this effect is 0.002 greater than our measured values, which have uncertainties of ±0.00025. The cause of the one low $^{178}Hf/^{177}Hf$ is not at present understood: such a sample would normally be re-analysed. Sample data for $^{145}Nd/^{144}Nd$ are entirely within uncertainty of the standard data, despite $^{147}Sm/^{144}(Sm + Nd)$ up to 0.135 and $^{147}Sm/^{149}Sm$ as low as 0.175 (static data only). Three static runs have $^{142}Nd/^{144}Nd$ slightly above the range observed in standards: these have $^{140}Ce/^{144}Nd > 1.5$, and their high $^{142}Nd/^{144}Nd$ may reflect the fact that uncertainty in the Ce correction is not propagated into the overall error.

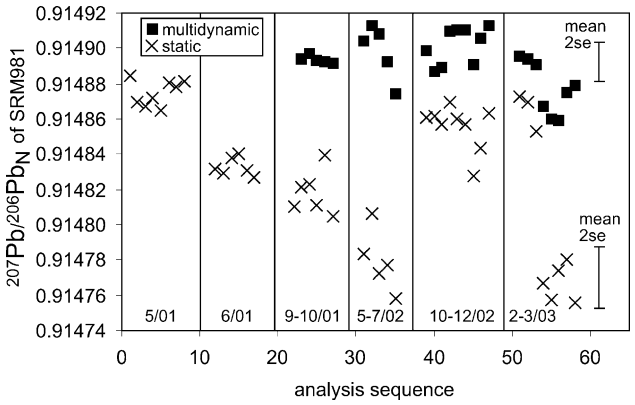

Fig. 7. Multidynamic $^{207}Pb/^{206}Pb$ IsoProbe analyses of SRM981 Pb solution between September 2001 and March 2003, compared with true static data (pre-9/01) and static results calculated from the multidynamic runs (post-8/01). Normalization to $^{208}Pb/^{206}Pb = 2.1677$ [8]. Error bar represents mean internal precision (2S.E.) of the analyses.

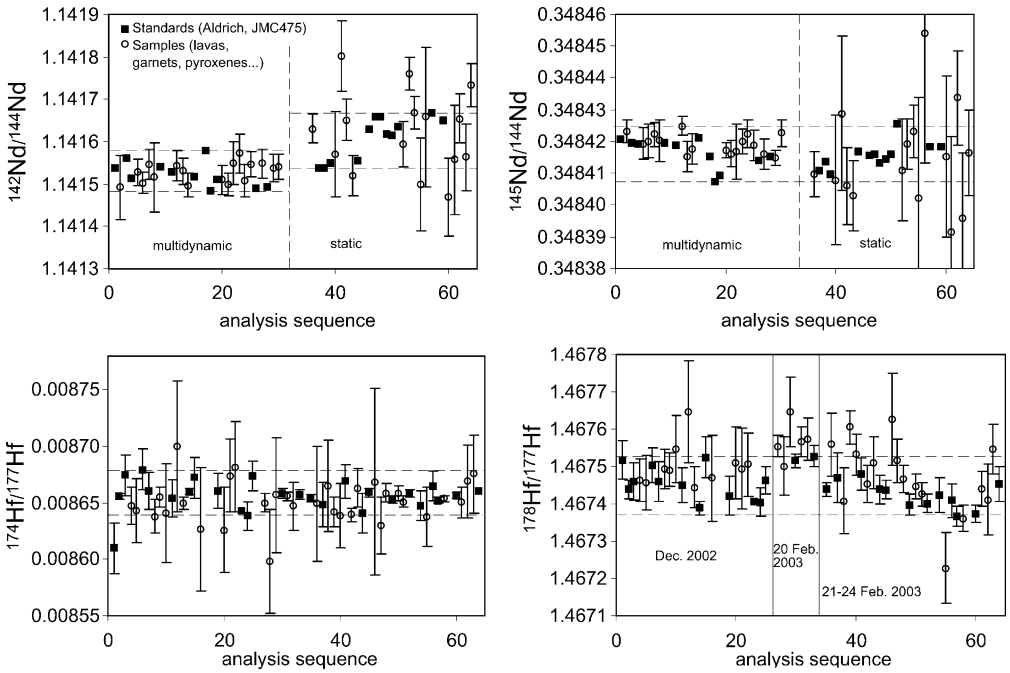

Fig. 8. Results of Hf and Nd non-radiogenic isotope ratios of spiked samples (open circles) and nearby standards (filled squares). Note that ratios have not been corrected for non-exponential mass bias or static-multidynamic differences. All Hf data are static, acquired on 6 days between 2/12/02 and 24/2/03, and include garnets, pyroxenes, amphiboles, lavas, and metamorphic rocks. Nd data include both multidynamic (largely lavas) and static runs, and were acquired on 2 days each for the multidynamic and static runs. Error bars represent 2S.E. internal precision. This is highly variable for samples because many analysed garnets have low signal intensities compared with the standard. The samples analysed for Nd include some with $^{140}Ce/^{144}Nd$ up to 3.8, $^{147}Sm/^{144}(Nd + Sm)$ up to 0.135, and $^{147}Sm/^{149}Sm$ as low as 0.175 (due to spike Sm).

5. Discussion

5.1. Origin of static-multidynamic differences

The poor long-term reproducibility of static Hf, Nd and Pb data since May 2001 (Figs. 2, 3 and 7; Tables 4 and 6) compared with multidynamic data might suggest a problem in the analyser. Faraday bucket deterioration would be expected to generate slow unidirectional change in the static ratios, such as seen for Pb between May 2001 and July 2002 (Fig. 7), but it cannot explain rapid reversals in the ratios, or steep changes in ratios within single days, as seen for Hf in August 2001 or April 2002. The reversals are not associated with analyser maintenance. The IsoProbe is also fitted with long-life Faraday buckets similar to those on our VG354 TIMS, and they have not been exposed to excessive ion beams. Variation in Faraday amplifier gains could also in principle explain the poor reproducibility of static data. These are usually measured between each day's work, but are reproducible to ~10 ppm, and when measured during the day, show no significant differences. At present therefore, the cause of this effect is unclear. The fact that many laboratories show similar or worse external precision for Hf than our static ratios (Table 6) suggests that we may not be the only laboratory with problems with our static ratios.

5.2. Origin of the correlations between mass-bias-corrected multidynamic ratios

The correlations between multidynamic ratios seen in Figs. 5 and 6 have a number of possible causes. Because they mostly have ^{177}Hf or ^{144}Nd as the denominator isotope, error in measurement of this might be thought to lead to positive correlations between ratios. Error in ^{177}Hf or ^{144}Nd measurement might be expected to lead to gradients of 1 in ln–ln ratio plots, but only if static ratios uncorrected for mass bias are plotted. Normalized static ratios will not show correlations with gradients of 1 in ln–ln plots since ^{177}Hf or ^{144}Nd forms part of the normalising ratio, and it is simple to show, for example, that a *negative* correlation is expected between normalized static $^{180}Hf/^{177}Hf$ and $^{178}Hf/^{177}Hf$ as a consequence of error in ^{177}Hf. The situation is more complex for multidynamic ratios, since the Eqs. (4)–(8) used to calculate them include several ion intensity measurements. It should be noted that the correlations seen in Figs. 5 and 6 are seen just as clearly in power law ratios as in ratios converted to exponential law using Eq. (1), so for simplicity we will consider only power law ratios. For the ratios defined by Eqs. (5) and (6), $^{176}Hf/^{177}Hf$ and $^{178}Hf/^{177}Hf$ have two common ^{177}Hf intensities in the denominator, so ^{177}Hf could cause a positive correlation between these ratios. In contrast, although there are also two common intensities in Eqs. (5) and (7), they appear in the numerator of one

and the denominator of the other. In this situation, any error in measuring individual intensities should lead to a negative $^{176}Hf/^{177}Hf$–$^{180}Hf/^{177}Hf$ correlation, not the positive one observed. Further, the peak jumping routines used allow calculation of several other multidynamic ratios. Several of these, e.g. $^{179}Hf/^{178}Hf$ normalized to $^{180}Hf/^{178}Hf$ using jumps 1 and 2, have no common ion intensities with other ratios (e.g. $^{178}Hf/^{177}Hf$ using jumps 2 and 3 to normalise to $^{179}Hf/^{177}Hf$) yet still show strong correlations (e.g. Fig. 5).

Similar correlations between multidynamic $^{143}Nd/^{144}Nd$ and $^{142}Nd/^{144}Nd$ were described by [9] using the same TIMS as used here, before upgrade to long-lasting buckets. Thirlwall [9] suggested that these could result from poor peak shape on the Faraday used to measure ^{146}Nd, used to normalise both ratios. This cannot explain the correlations here, since they are observed in multidynamic ratio pairs with no common ion intensities.

The correlations observed are also similar to those reported by [5], who saw strong correlations between static and multidynamic Nd isotopic ratios normalized to $^{146}Nd/^{144}Nd = 0.7219$. This was attributed to a non-exponential component to the mass bias, and was also seen in the departure from expected exponential-law gradients of the correlations between $\ln(^{x}Nd/^{144}Nd_m)$ and $\ln(^{146}Nd/^{144}Nd_m)$, where the subscript m refers to ratios uncorrected for mass bias. A similar explanation for the correlations observed here is suggested by the broad dependence of the normalized isotope ratios on extraction potential (e.g. Fig. 4, post-upgrade), the differences between soft and hard extraction data often run on the same day (Figs. 5 and 6), and broad residual correlations between normalized multidynamic ratios and the measured static $^{179}Hf/^{177}Hf$ or $^{146}Nd/^{144}Nd$ (e.g. Fig. 4). Unlike [5], the observed long-term gradients for mass-bias-uncorrected ratios on ln–ln plots for Hf are similar to expected exponential-law gradients (Table 5), but there is a lot of scatter reflected in poor MSWD values, which is at least in part due to the unavoidable use of static ratios for this purpose. Standards run over a short time period (e.g. September 2003, Table 5), in which the static:multidynamic differences are expected to change little, can have rather different gradients on ln-ln plots, but these usually have large errors because of limited change in mass bias over short time periods. Gradients that are inconsistent with exponential law on ln-ln plots of mass-bias-uncorrected ratios inevitably require that there will be correlations between ratios normalized using the exponential law. It can be shown that, for example, if k_i and F_i are the observed gradient and predicted exponential gradient on plots of $\ln(^{i}Hf/^{177}Hf)$ versus $\ln(^{179}Hf/^{177}Hf)$ before normalisation, then after normalisation there will be gradients of $(k_i - F_i)/(k_{178} - F_{178})$ on graphs of normalized $\ln(^{i}Hf/^{177}Hf)$ versus $\ln(^{178}Hf/^{177}Hf)$. The predicted gradients on plots of (normalized) multidynamic ratios are the same, but only if the static measured ratios used to calculate k were measured during a short time period in which there was no change in the difference between static and multidynamic ratios. Unfortunately, using only data from a short time period yields uncertainties on the gradients that preclude useful comparison. However, it appears that there are consistent long-term relationships between the multidynamic ratios which strongly imply that both Hf and Nd mass bias on the IsoProbe are not fully described by the exponential law.

Maréchal et al. [20] noted that the exponential law is a special case of a general power law of mass bias. In this the mass bias affecting a ratio i/j is taken to be a function of $M_i^q - M_j^q$, where exponent q can be varied so as to describe best the observed mass bias. If our IsoProbe data were to be better described by a non-exponential form of the general power law, then it is inevitable that correlations such as Figs. 5 and 6 would result between ratios corrected using the exponential law. The gradients of such correlations on plots of $\ln(^{i}Hf/^{177}Hf)$ versus $\ln(^{j}Hf/^{177}Hf)$ can be shown to be:

$$\text{Gradient} = \frac{[\ln(M_i/M_{177})/\ln(M_{179}/M_{177}) - (M_i^q - M_{177}^q)/(M_{179}^q - M_{177}^q)]}{[\ln(M_j/M_{177})/\ln(M_{179}/M_{177}) - (M_j^q - M_{177}^q)/(M_{179}^q - M_{177}^q)]}$$

Remarkably, the gradients are not very dependent on q, except if q is closer to zero than ± 0.0001, which is effectively exponential law. For q between $+5$ and -5 (at which limits normalized static ratios are wildly inaccurate), the uncertainty in the expected gradients reported in Table 7 is less than 10%. It is quite clear from Table 7 that the observed correlation gradients for Hf and Nd multidynamic IsoProbe ratios are not the result of mass bias following any general power law with constant q. However, the gradients calculated for Nd fit those reported for TIMS power-law-normalized ratios by [9].

5.3. Multidynamic TIMS-IsoProbe comparisons

Vance and Thirlwall [5] described two additional characteristics of non-exponential components to Nd mass bias. They observed worse external precision and lower than expected isotope ratios the further the average mass of the measured ratio was from that of the normalising ratio $^{146}Nd/^{144}Nd$, with $^{142}Nd/^{144}Nd$ and $^{150}Nd/^{144}Nd$ yielding values 300–700 ppm lower than the TIMS natural Nd isotope ratios of [7]. Fig. 9 compares 2S.D. external precision and deviations in IsoProbe Nd and Yb ratios from our new multidynamic TIMS ratios (Tables 3 and 4), as a function of the average mass of a ratio relative to the normalising ratios $^{146}Nd/^{144}Nd$ and $^{174}Yb/^{172}Yb$ respectively. In multidynamic calculations, there is some difficulty in determining the difference between the average mass of the normalized and normalising ratios. With the definition of $^{150}Nd/^{144}Nd$ of Eq. (9), these averages are 149 and 147, respectively,

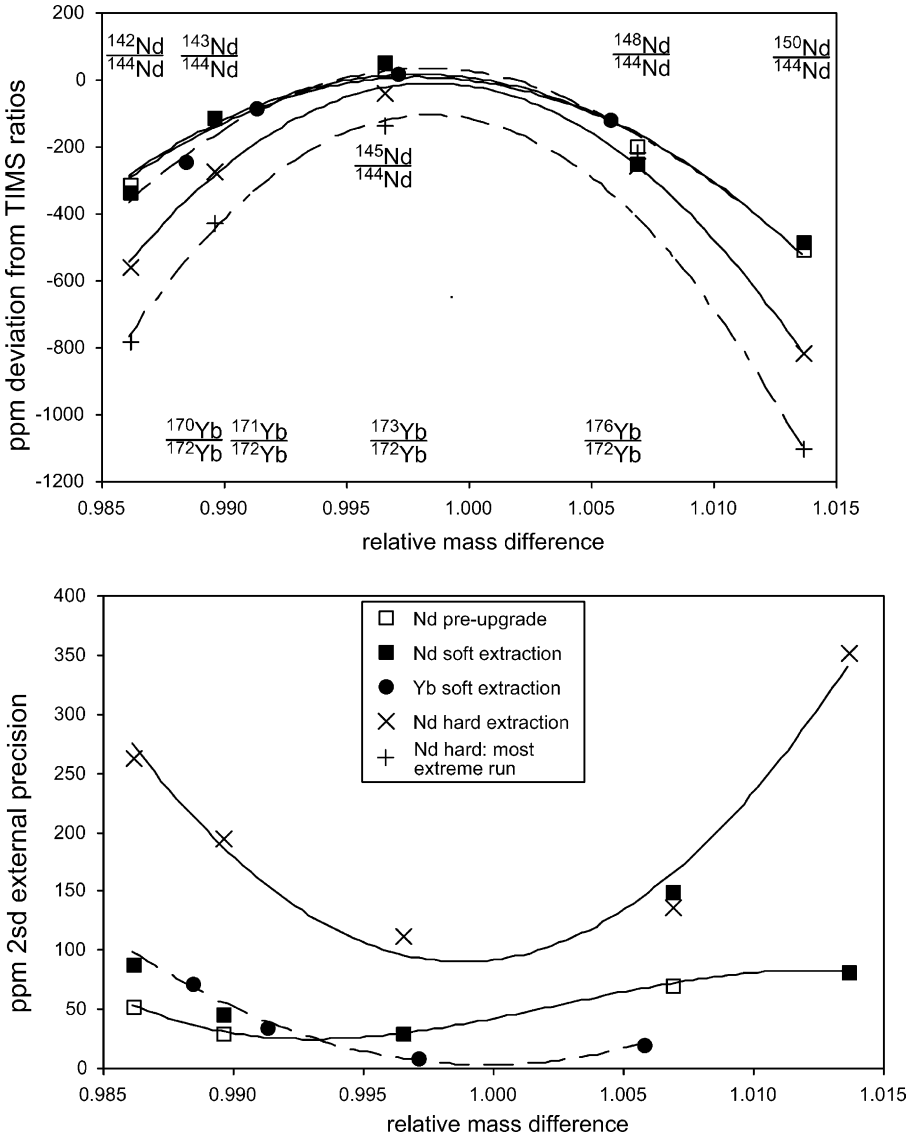

Fig. 9. External precision (2S.D.) and ppm deviation from TIMS ratios of mean Nd and Yb multidynamic IsoProbe data, as a function of proportional mass difference between measured and normalising isotope ratios.

giving the same mass difference as $^{150}Nd/^{144}Nd$ normalized directly in static mode to $^{146}Nd/^{144}Nd$. However, Eq. (8) used to calculate $^{148}Nd/^{144}Nd$ and $^{176}Yb/^{172}Yb$ is actually measuring $^{176}Yb/^{174}Yb$ normalized to $^{174}Yb/^{172}Yb$, suggesting a mass difference of 2 (=175–173), but the expression is algebraically identical to the standard static calculation of $^{176}Yb/^{172}Yb$ where the mass difference is only 1. We can avoid this problem by comparing ratios that are calculated in a similar way e.g. $^{176}Hf/^{177}Hf$ and $^{171}Yb/^{172}Yb$ are calculated using similar expressions to $^{143}Nd/^{144}Nd$.

Fig. 9 demonstrates that *both* Nd and Yb multidynamic ratios show systematically greater deviation from the TIMS ratios and in general worse external precision the greater the difference in average mass between the normalized and normalising ratios, as shown for static Nd by [5]. The data are fit well by second-order polynomial curves which crest or trough at $^{145}Nd/^{144}Nd$ and $^{173}Yb/^{172}Yb$. Only $^{148}Nd/^{144}Nd$ does not fit the curves too well, with the soft extraction data having unusually poor external precision and a much larger deviation from TIMS than expected. The post-upgrade hard extraction Nd data show much greater average deviation from TIMS values than the soft extraction data, but this is the average of a large range that overlaps soft extraction data (Fig. 6). Individual runs at the extremes of this range show deviation curves of very similar shape to the mean in Fig. 9.

The similarity in curve shape between all data sets, and the essentially identical curves for Nd and Yb soft extraction data, require a common cause for both the

Table 9
Multidynamic IsoProbe Nd, Yb and Hf ratios mass-bias-corrected using the general power law

	Using constant q					
	$^{142}Nd/^{144}Nd$	$^{143}Nd/^{144}Nd$	$^{145}Nd/^{144}Nd$	$^{148}Nd/^{144}Nd$	$^{150}Nd/^{144}Nd$	q
Preferred TIMS	**1.141877 ± 15**	**0.511413 ± 08**	**0.348408 ± 05**	**0.241576 ± 06**	**0.236491 ± 10**	0
Pre-upgrade	1.141879 ± 62	0.511414 ± 15	0.348404 ± 10	0.241599 ± 19	0.236441 ± 21	–0.63
Soft extraction	1.14188 ± 12	0.511419 ± 23	0.348410 ± 11	0.241593 ± 41	0.236452 ± 19	–0.70
Hard extraction	1.14188 ± 36	0.511380 ± 108	0.348370 ± 38	0.241643 ± 47	0.236422 ± 96*	–1.45
WR	1.141878	–	0.348411	0.241580	0.236445	–0.23
	$^{170}Yb/^{172}Yb$	$^{171}Yb/^{172}Yb$	$^{173}Yb/^{172}Yb$	$^{176}Yb/^{172}Yb$		
Preferred TIMS*	**0.139903 ± 07**	**0.655345 ± 15**	**0.736251 ± 22**	**0.579397 ± 19**		0
Soft extraction*	0.139903 ± 10	0.655346 ± 21	0.736242 ± 06	0.579461 ± 12		–0.58
	$^{176}Hf/^{177}Hf$	$^{178}Hf/^{177}Hf$	$^{180}Hf/^{177}Hf$			
All multidynamic	0.282182 ± 22	1.46730 ± 8	1.88697 ± 17			–0.63
	Using q optimised based on the $^{142}Nd/^{144}Nd$ of each run					
		$^{143}Nd/^{144}Nd$	$^{145}Nd/^{144}Nd$	$^{148}Nd/^{144}Nd$	$^{150}Nd/^{144}Nd$	
Pre-upgrade	–	0.511413 ± 10	0.348403 ± 10	0.241598 ± 22	0.236440 ± 19	
Soft extraction	–	0.511418 ± 16	0.348410 ± 10	0.241593 ± 25	0.236451 ± 24	
Hard extraction	–	0.511379 ± 52	0.348371 ± 49	0.241641 ± 62	0.236421 ± 56	

All uncertainties are 2S.D. q is the exponent in the general power law normalisation equation [20]. WR, Wombacher and Rehkämper (2003) [6]. Normalization for mass bias is to $^{179}Hf/^{177}Hf = 0.7325$, $^{174}Yb/^{172}Yb = 1.4519785$, $^{146}Nd/^{144}Nd = 0.7219$, and (*) it is unlikely that this is a good estimate of the true composition of Yb (Section 3.5).

inaccuracy and relatively poor reproducibility of the exponential-law-normalized ratios. The mass dependence of both strongly suggests an origin in mass discrimination, as proposed by [5]. Wombacher and Rehkämper [6] report Nd data from Nu Plasma instruments at ETH Zürich that show some similarities to our data when exponential-law normalisation is used (Table 4). They show that they can achieve accurate isotope ratios relative to the TIMS ratios of [7] using general power law with exponent $q \approx -0.23$, though they observed that during routine operation the optimum value of q could vary from -0.2 to -0.4 between analytical sessions. Table 9 reports their GPL-corrected data, together with our Yb data and the three Nd datasets shown in Fig. 6, corrected using GPL with constant q. A GPL exponent q of about -0.63 generates normalized Nd and Yb isotope ratios that are very close to TIMS values for soft extraction and pre-upgrade data. The main exceptions are $^{148}Nd/^{144}Nd$ and $^{176}Yb/^{172}Yb$, which are respectively 95 and 111 ppm high, and $^{150}Nd/^{144}Nd$, which is 165–211 ppm low. The theoretical ppm difference between GPL and exponential law is very similar for $^{148}Nd/^{144}Nd$ and $^{150}Nd/^{144}Nd$ because of the way that multidynamic $^{150}Nd/^{144}Nd$ is calculated (Eq. (9)), but observed $^{150}Nd/^{144}Nd$ is seen to have a much greater deviation from TIMS than $^{148}Nd/^{144}Nd$ (Fig. 9), closer to the GPL-exponential difference expected for $^{150}Nd/^{144}Nd$ calculated in static mode.

The fact that similar q exponents in the general power law yield *both* Nd and Yb ratios that are much more accurate than those corrected using the exponential law is strong support for the views of [6]. However, as also observed by these authors, the GPL correction fails to improve the external precision. It also cannot generate accurate Nd ratios for data collected in hard extraction since the instrument upgrade (Table 9). Table 9 also reports GPL-corrected data for Nd in which q is optimised to give the TIMS $^{142}Nd/^{144}Nd$ value for each sample. This does not improve the accuracy further but does improve the external precision of some ratios, particularly $^{143}Nd/^{144}Nd$. This would imply large variation in the mass bias law (e.g. $q = -1.0$ to -1.8) on a single day in hard extraction mode.

The Nd and Yb datasets cover the same period and methodologies in which the multidynamic Hf data were acquired. Since soft extraction Yb and Nd data require much the same GPL exponent to produce accurate ratios, it is highly likely that the soft extraction Hf data require a similar exponent, and a rather more negative exponent for hard extraction data, to produce accurate Hf ratios. Table 9 also reports our multidynamic Hf ratios corrected using GPL with $q = -0.63$. Again, the GPL correction worsens the external precision, but strongly suggests that true $^{176}Hf/^{177}Hf$ and $^{180}Hf/^{177}Hf$ are significantly higher than the multidynamic ratios we report in Table 6.

5.4. Empirical corrections

An empirical correction to TIMS and MC–ICP–MS $^{143}Nd/^{144}Nd$ data based on the slope of the observed correlation between exponential-law-normalized $^{143}Nd/^{144}Nd$ and $^{142}Nd/^{144}Nd$ was proposed by [9,5]. In reality, the exponential law itself is an empirical correction, proposed by [26] as a law that described well TIMS Ca isotope fractionation. Consequently, there can be no philosophical objection to use of an empirical relationship. The method of [5], using regression against $^{142}Nd/^{144}Nd$, has similarities to the method used in Table 9 where the GPL exponent is optimised for each analysis to yield

the TIMS value for $^{142}Nd/^{144}Nd$. However, these methods break down when applied to the Nd data obtained in hard extraction since the instrument upgrade. These data still show strong post-GPL-normalisation correlations between several ratios, in particular $^{143}Nd/^{144}Nd$ and $^{145}Nd/^{144}Nd$. This led us to investigate relationships between exponential-law-normalized ratios in three dimensions, using the planar regression facility of Isoplot [27]. All but one of our 64 multidynamic Nd analyses lie nearly within error of a plane in $^{143}Nd/^{144}Nd$-$^{142}Nd/^{144}Nd$-$^{145}Nd/^{144}Nd$ space (MSWD 1.7). Using the TIMS ratios for $^{145}Nd/^{144}Nd$ and $^{142}Nd/^{144}Nd$ we define a correction equation for $^{143}Nd/^{144}Nd$:

$$\left(\frac{^{143}Nd}{^{144}Nd}\right)_{corr} = \left(\frac{^{143}Nd}{^{144}Nd}\right)_{meas} + 0.210 \times \left(1.141877 - \left(\frac{^{142}Nd}{^{144}Nd}\right)_{meas}\right) + 0.94 \times \left(0.348408 - \left(\frac{^{145}Nd}{^{144}Nd}\right)_{meas}\right)$$

Uncertainties on the gradients are ±0.013 and ±0.13 for $^{142}Nd/^{144}Nd$ and $^{145}Nd/^{144}Nd$, respectively. The correction yields a final mean $^{143}Nd/^{144}Nd$ from our data of 0.511420 ± 13 (2S.D., $N = 63$), within error of the TIMS ratio, and a worst external precision of ±0.0000015 for the hard extraction dataset. The external precision on the corrected data is 1.6× the mean internal precision. It is notable that the coefficient for $^{142}Nd/^{144}Nd$ is very similar to the TIMS gradient reported by [9]. We suggest that the success of this planar regression is because $^{143}Nd/^{144}Nd$ is bracketed by $^{142}Nd/^{144}Nd$ and $^{145}Nd/^{144}Nd$. Planar regression of other sets of three Nd ratios is somewhat less successful, with MSWD of 3.2 for $^{142}Nd/^{144}Nd$–$^{143}Nd/^{144}Nd$–$^{150}Nd/^{144}Nd$ and MSWD 7.8 for $^{142}Nd/^{144}Nd$–$^{148}Nd/^{144}Nd$–$^{150}Nd/^{144}Nd$.

The linear regressions for $^{176}Hf/^{177}Hf$ against $^{178}Hf/^{177}Hf$ and $^{180}Hf/^{177}Hf$ (Table 7) permit empirical regressions for Hf as well. A linear correction to the mean analysed $^{178}Hf/^{177}Hf$ improves external precision of $^{176}Hf/^{177}Hf$ to ±0.000014 (2S.D.) from ±0.000018 without, but a correction based on $^{180}Hf/^{177}Hf$ does not make a significant improvement due to the displacement of the 5–9/02 data in $^{180}Hf/^{177}Hf$ (Fig. 5). Planar regressions do not improve the Hf data.

5.5. Comparison with other MC–ICP–MS laboratories

Nonradiogenic MC–ICP–MS Nd ratios were reported by [1,6], using P54 and Nu Plasma machines, respectively. As discussed above, Wombacher and Rehkämper [6] report data similar to but not so extreme as ours. The data of [1] have external precision intermediate between our soft and hard extraction data, and $^{150}Nd/^{144}Nd$ at least 200 ppm lower than our new TIMS value. Despite worse external precision, the IsoProbe Yb ratios of [17] are very similar to our IsoProbe ratios, with $^{170}Yb/^{172}Yb$ and $^{176}Yb/^{172}Yb$ distinctly lower than our TIMS ratios, as are the $^{171}Yb/^{172}Yb$ and $^{176}Yb/^{172}Yb$ of [18] (Table 3). Published Hf ratios for most laboratories have external precision similar to or worse than our multidynamic data (Table 6), suggesting either worse counting statistics, problems with static data comparable to ours, or non-exponential effects. Reported ratios for JMC475 from most other laboratories are broadly similar to, and in most cases lower than our multidynamic ratios (Table 6). Slightly higher $^{176}Hf/^{177}Hf$ is only reported by [28] and higher $^{180}Hf/^{177}Hf$ is only reported by [29]. There are only two possible reasons for this:

- The only previously published multidynamic data sets are the TIMS data of [30] and the MC–ICP–MS data of [16], and in the latter it appears that only $^{176}Hf/^{177}Hf$ was measured in multidynamic mode. Our implied higher $^{180}Hf/^{177}Hf$ is outside the 2S.D. error range reported by [30]. However, the remaining published Hf data are static and thus not independent of assumed cup efficiencies.
- Other MC–ICP–MS laboratories may have a similar or even greater extent of non-exponential mass bias as the Royal Holloway IsoProbe. This may pass unnoticed because the absolute Hf isotope ratios are not well-known.

Since there is no particular reason why non-unity cup efficiencies should yield low static data from eight out of nine laboratories, it seems likely that almost all MC–ICP–MS laboratories are measuring less than the true isotopic ratios for $^{176}Hf/^{177}Hf$ and $^{180}Hf/^{177}Hf$ as a result of unidentified non-exponential mass bias. Similar problems were reported for Ru isotope analysis on a Nu Plasma by [31]. While non-exponential mass bias will only contribute to poor external precision over a limited mass range, there are several situations where major error can be introduced by assuming exponential law. Wherever correction is needed over a large mass range, for example in light stable isotope analysis, or to correct interfering species to the mass bias of the analyte, large errors may be introduced. Correction of Yb interference on Hf during laser ablation analysis is one example of mass bias correction over a large mass range. Excessive error propagation can be introduced into double spike mass bias corrections if a double spike is calibrated when the extent of non-exponential mass bias was different to that when samples were analysed. Finally, we have shown that the extent of non-exponential mass bias can vary substantially in a single day, and thus corrections to measured sample isotope ratios based on standards may not always be appropriate.

6. Summary

- New TIMS reference values for Nd and Yb isotope ratios obtained by multidynamic techniques with exponential-law normalisation are presented in Table 9.

- Nd and Yb obtained by similar multidynamic techniques on an IsoProbe MC–ICP–MS are systematically more inaccurate the further the average mass of a ratio is from that of the normalising ratio. Mass bias correction using the general power law [20] with an exponent $q = -0.63$ yields accurate IsoProbe Yb and Nd ratios for data sets acquired in soft extraction mode or prior to the interface upgrade, apart from some ambiguities in applying GPL to multidynamic data.
- Application of the same GPL exponent to Hf data requires that $^{176}Hf/^{177}Hf$ and $^{180}Hf/^{177}Hf$ for standard JMC475 are greater than all values so far reported by MC–ICP–MS, and strongly suggests that all other MC–ICP–MS instruments have similar non-exponential mass bias to the IsoProbe in this mass range.
- Drift in IsoProbe isotopic ratios with time reflects change in the non-exponential component of mass bias through time and also change in apparent cup efficiency. GPL normalisation can not account for the former drift, and routine use of GPL normalisation is not advisable. Some empirical corrections appear to be robust on our IsoProbe, but these need to be investigated using multidynamic results from other machines. Drift in apparent cup efficiency is demonstrated by sometimes very rapid large drift in static ratios unaccompanied by change in multidynamic ratios. Based on broadly similar external precisions for other instruments, often over shorter time periods, it is likely that similar causes of temporal drift apply elsewhere.
- Static analyses relative to standards can only yield high quality data if the standard ratios are known and if the causes of drift are accurately corrected by the use of standards. We recommend that multidynamic analyses of standards should be used periodically to constrain the causes of secular ratio drift.
- Double spike correction procedures require that accurate isotope ratios are being measured. Users of double spikes should be aware of pitfalls resulting from secular ratio drift.

Acknowledgements

Part of this work was funded by NERC under grant GR3/13160 to Prof. J. Platt (University College London) and MFT. Detailed reviews by Mark Rehkämper and Joel Baker were most helpful. We are grateful to Dawn Munday, Barbara Seth, Erwan Bourdon, Derek Vance, Corey Archer and Clinton Roberts for some standard analyses and assistance with laboratory maintenance. Preparation of this paper was supported by a Royal Society/Leverhulme Trust Senior Research Fellowship to MFT.

References

[1] B. Luais, P. Telouk, F. Albarède, Geochim. Cosmochim. Acta 61 (1997) 4847.
[2] J.D. Woodhead, J.M. Hergt, J.P. Davidson, S.M. Eggins, Earth Planet. Sci. Lett. 192 (2001) 331.
[3] M. Rehkämper, K. Mezger, J. Anal. At. Spectrom. 15 (2000) 1451.
[4] F. Albarède, Geochim. Cosmochim. Acta 66 (2002) A1.
[5] D. Vance, M.F. Thirlwall, Chem. Geol. 185 (2002) 227.
[6] F. Wombacher, M. Rehkämper, J. Anal. At. Spectrom. 18 (2003) 1371.
[7] G.J. Wasserburg, S.B. Jacobsen, D.J. DePaolo, M.T. McCulloch, T. Wen, Geochim. Cosmochim. Acta 45 (1981) 2311.
[8] M.F. Thirlwall, Chem. Geol. 184 (2002) 255.
[9] M.F. Thirlwall, Chem. Geol. 94 (1991) 85.
[10] Z. Palacz, C. Haines, P. Turner, Micromass Technical Note 307 (1997).
[11] M.F. Thirlwall, J. Anal. At. Spectrom. 16 (2001) 1121.
[12] B. Seth, M.F. Thirlwall, S.L. Houghton, C.-A. Craig, J. Anal. At. Spectrom. 18 (2003) 1323.
[13] C.L. Harper, L.E. Nyquist, C.Y. Shih, Meteoritics 25 (1990) 369.
[14] S. Weyer, C. Münker, M. Rehkämper, K. Mezger, Chem. Geol. 187 (2002) 295.
[15] M.T. McCulloch, K.J.R. Rosman, J.R. DeLaeter, Geochim. Cosmochim. Acta 41 (1977) 1703.
[16] J. Blichert-Toft, C. Chauvel, F. Albarède, Contrib. Mineral. Petrol. 127 (1997) 248.
[17] N.-C. Chu, R.N. Taylor, V. Chavagnac, R.W. Nesbitt, R.M. Boella, J.A. Milton, C.R. German, G. Bayon, K. Burton, J. Anal. At. Spectrom. 17 (2002) 1567.
[18] I. Segal, L. Halicz, I. Platzner, J. Anal. At. Spectrom. 18 (2003) 1217.
[19] T.-L. Chang, M.-T. Zhao, W.-J. Li, J. Wang, Q.-Y. Qian, Int. J. Mass Spectrom. 177 (1998) 131.
[20] C.N. Maréchal, P. Telouk, F. Albarède, Chem. Geol. 156 (1999) 251.
[21] T. Tanaka, S. Togashi, H. Kamioka, H. Amakawa, H. Kagami, T. Hamamoto, M. Yuhara, Y. Orihashi, S. Yoneda, H. Shimizu, T. Kunimaru, K. takahashi, T. Yanagi, T. Nakano, H. Fujimaki, R. Shinjo, Y. Asahara, M. Tanimizu, C. Dragusanu, Chem. Geol. 168 (2000) 279.
[22] G. Caro, B. Bourdon, J.-L. Birck, S. Moorbath, Nature 423 (2003) 428.
[23] S. Graham, D.D. Lambert, S.R. Shee, N.J. Pearson, Chem. Geol. 186 (2002) 215.
[24] A. Stracke, A. Zindler, V.J.M. Salters, D. McKenzie, J. Blichert-Toft, F. Albarède, K. Grönvold, Geochem. Geophys. Geosyst. 4 (2003) 2001GC000201.
[25] M.F. Thirlwall, Chem. Geol. 163 (2000) 299.
[26] W.A. Russell, D.A. Papanastassiou, T.A. Tombrello, Geochim. Cosmochim. Acta 42 (1978) 1075.
[27] K.R. Ludwig, Isoplot USGS (2001).
[28] I.C. Kleinhanns, K. Kreissig, B.S. Kamber, T. Meisel, T.F. Nägler, J.D. Kramers, Anal. Chem. 74 (2002) 67.
[29] Y. Amelin, D.-C. Lee, A.N. Halliday, Geochim. Cosmochim. Acta 64 (2000) 4205.
[30] R.K. Stevenson, P.J. Patchett, Geochim. Cosmochim. Acta 54 (1990) 1683.
[31] H. Becker, C. Dalpe, R.J. Walker, Analyst 127 (2002) 775.
[32] E.E. Scherer, K.L. Cameron, J. Blichert-Toft, Geochim. Cosmochim. Acta 64 (2000) 3413.
[33] C. Münker, S. Weyer, E. Scherer, K. Mezger, Geochem. Geophys. Geosyst. 2 (2001) 2001GC000183.
[34] D. Ulfbeck, J. Baker, T. Waight, E. Krogstad, Talanta 59 (2003) 365.
[35] W.L. Griffin, N.J. Pearson, E. Belousova, S.E. Jackson, S.Y. O'Reilly, E. van Acherbergh, S.R. Shee, Geochim. Cosmochim. Acta 64 (2000) 133.
[36] R. Anczkiewicz, J. Platt, M.F. Thirlwall, J. Wakabayashi, Earth Planet. Sci. Lett. (2004), in press.